

UNIVERSITY OF OKLAHOMA

GRADUATE COLLEGE

SURFACTANT-ONLY EOR FOR HIGH SALINITY BRINE

A DISSERTATION

SUBMITTED TO THE GRADUATE FACULTY

in partial fulfillment of the requirements for the

Degree of

DOCTOR OF PHILOSOPHY

By

MAHESH BUDHATHOKI

Norman, Oklahoma

2015

SURFACTANT-ONLY EOR FOR HIGH SALINITY BRINE

A DISSERTATION APPROVED FOR THE  
SCHOOL OF CHEMICAL, BIOLOGICAL AND MATERIALS ENGINEERING

BY

---

Dr. Jeffrey H. Harwell, Chair

---

Dr. Bor-Jier (Ben) Shiau

---

Dr. Ahmad Jamili

---

Dr. Edgar A. O' Rear III

---

Dr. Lance L. Lobban

© Copyright by MAHESH BUDHATHOKI 2015  
All Rights Reserved.

I dedicate my dissertation work to my family and friends who supported me throughout the process. My grandparents who shared their experience and wisdom with me in a loving and caring way. My parents whose love and words of encouragement always motivated me and helped me get this far. My brother who always inspired me through his good work ethic, humility and peaceful nature. My committee members who gave me their time and expertise and helped me develop my technology skills. My friends who helped me and made me laugh in these years. My girlfriend who always supported me, cared for me and was there for me in every pitfalls. Thank you for being my best cheerleader.

## **Acknowledgements**

The author would like to give special thanks to Oklahoma Economic Development Generating Excellence (Grant number: EDGE09-013-FP) and Research Partnership to Secure Energy for America (RPSEA project number: 11123-24) for financially supporting this research. The authors would also like to thank Sasol North America, Lake Charles, LA for providing extended surfactants and Mid-Con Energy Inc., Tulsa, Oklahoma for providing reservoir brine and crude oil. Finally, the author would like to thank Bruce L. Roberts, Tzu-ping Hsu, Prapas Lohateeraparp, Javen Weston, Michael Bendrick, Ajay Raj, Wei Wan, Sangho Bang, Shengbo Wang, Danielle Baker, Miguel Gonzalez Borja, Felipe Anaya Saltarin, and many others who helped him throughout this research.

## Table of Contents

Acknowledgements .....	iv
List of Tables .....	viii
List of Figures.....	x
Abstract.....	xiii
CHAPTER 1: Introduction.....	1
CHAPTER 2: Design of an Optimal Middle Phase Microemulsion for Ultra High Saline Brine using Hydrophilic Lipophilic Deviation (HLD) Method .....	5
Introduction .....	5
Hydrophilic Lipophilic Deviation (HLD) Concept .....	8
Experimental.....	11
Materials .....	11
Microemulsion Phase Study.....	13
Stability Study of Surfactant Solution.....	14
Equilibrium IFT Measurement.....	14
One-Dimensional Sand-Pack Test.....	14
Results and Discussion.....	15
Determination of K and Cc-values.....	15
Temperature Dependence of Extended and Conventional Anionic Surfactants .....	22
Prediction of Surfactant/Co-Surfactant Ratio.....	23
Phase Behavior Study and Surfactant Stability Test .....	25
IFT Measurements and Optimal Point .....	26
Accuracy of the HLD Equation .....	28

Sand Packed Experiment .....	29
Conclusion .....	30
CHAPTER 3: Single Well Field Feasibility of Surfactant-Only Flooding in Extreme	
Saline Brine Reservoir .....	31
Introduction .....	31
Background: Single Well Tracer Test (SWCTT) .....	33
Experimental .....	35
Materials .....	35
Reservoir Information .....	36
Sand Pack Study .....	36
Partitioning Coefficient and Hydrolysis Rate Constant .....	37
SWCTT Field Operation .....	38
SWCTTs Data Interpretation Method .....	39
Results and discussions .....	41
Surfactant Formulations .....	41
Sand Pack Experiments .....	42
Equilibrium Partitioning Tracer Coefficient, $K$ .....	46
Field Test Results Interpretation .....	47
Conclusion .....	49
CHAPTER 4: Improved Oil Recovery by Reducing Surfactant Adsorption with	
Polyelectrolyte in High Saline Brine .....	51
Introduction .....	51
Experimental .....	54

Materials .....	54
Equilibrium Adsorption Study .....	56
Dynamic Adsorption Study .....	56
Sand Pack Experiments .....	57
Results and discussions .....	57
Equilibrium Adsorption of Surfactant without Polyelectrolyte.....	57
Equilibrium Adsorption of Polyelectrolytes without Surfactant .....	59
Equilibrium Adsorption of Surfactant with Polyelectrolyte.....	60
Dynamic Adsorption of Surfactant without Polyelectrolyte .....	63
Dynamic Adsorption of Surfactant with Polyelectrolyte .....	65
Oil Mobilization in Sand Packs without Polyelectrolytes .....	67
Oil Mobilization in Sand Packs with Polyelectrolytes .....	69
Conclusions .....	72
CHAPTER 5: Conclusions, Implications and Future Works .....	74
References .....	78



## List of Tables

Table 1. Surfactant Properties .....	12
Table 2. Reservoir Brine Analysis. Analysis Conducted by Red River Laboratory, Oklahoma City, OK.....	12
Table 3. Characteristic of the crude oil. Analysis conducted by Harris Testing Laboratory, Houston, TX .....	12
Table 4. Effect of surfactant structure on optimal salinity; $S^*$ is in g of NaCl/100 ml solution and total surfactant concentration is 0.1M.....	15
Table 5. Experimentally obtained K-values and $C_c$ -values of extended and conventional surfactants unless otherwise noted. $C_c^*$ is the $C_c$ -value calculated by using group contribution correlation .....	18
Table 6. Calculated required or predicted $C_c$ to produce optimal Type III microemulsion of the site specific crude and brine at the reservoir conditions .....	24
Table 7. Predicted mole fraction (x) and weight fraction (y) of the binary mixtures to produce optimal type III microemulsions.....	24
Table 8. Phase behavior studies, IFT measurement, and concentration of Steol Cs460 at optimal for each surfactant mixture. The concentration of extended surfactants at optimal is 0.25 wt %.....	25
Table 9. Accuracy validation of the HLD equation .....	28
Table 10. Formation Brine Analysis .....	36
Table 11. Field operational steps and amount of chemicals injected, 1 PV = 85 bbls ...	38
Table 12. Summary of sand pack studies .....	45
Table 14. Simulation Matching Parameters. Software: CMG-STARS .....	49

Table 15. Composition of Brea Sandstone and Ottawa Sand. Information provided by  
supplier ..... 55

## List of Figures

Figure 1. Effect of High TDS on homogeneous single phase micellar solution .....	6
Figure 2. Plot of $\ln(S^*)$ Vs EACN to determine the K and Cc of the extended surfactants.....	17
Figure 3. Effect of surfactant mixture (AMA and SDS or Steol Cs460) composition on overall salinity; Surfactant 2 is SDS or Steol Cs460. Oil phase is Limonene.....	20
Figure 4. Phase behavior: Steol Cs460 scan for $C_8-(PO)_4-(EO)_1-SO_4Na$ (0.25 wt. %) at the reservoir temperature ( $52^\circ C$ ) with crude oil.....	25
Figure 5. Equilibrium IFT measurements of the binary mixtures (extended surfactant, 0.25 wt. % + Steol Cs460) with the reservoir crude oil at $52^\circ C$ .....	27
Figure 6. Sand packed study: Effect of 1 PV, 0.75 wt. % surfactant slug consisting mixture of $C_{10}-(PO)_4-(EO)_1-SO_4Na$ and Steol Cs460 on cumulative oil recovery and Sor reduction. ....	29
Figure 7. Equilibrium IFT measurements of the binary mixtures ( $C_8-(PO)_4-(EO)_1-SO_4Na$ , 0.25 wt % + SAES) with the reservoir crude oil at $52^\circ C$ .....	41
Figure 8. Effect of surfactant concentration on cumulative oil recovery and oil break through. Post water flooding surfactant injection (1 PV).....	42
Figure 9. Effect of surfactant concentration on oil bank position. A) 1 PV, 0.25 wt% B) 1 PV, 0.50 wt% C) 1 PV, 0.75 wt%. Fluid injection rate: 0.3 ml/min. ....	43
Figure 10. Effect of surfactant slug size on cumulative oil recovery .....	44
Figure 11. Ethylformate hydrolysis rate constant study conducted at $52^\circ C$ .....	46
Figure 12. Pre Surfactant SWCTT tracer concentration profile; single layer fitting. Software: CMG-STARS.....	47

Figure 13. Post Surfactant SWCTT tracer concentration profile; single layer fitting. Software: CMG-STARS.....	48
Figure 14. Surfactant Adsorption Isotherm .....	51
Figure 15. Equilibrium surfactant adsorption without polyelectrolyte in two different salinity environment .....	58
Figure 16. Equilibrium PSS adsorption without surfactant on Brea Sandstone at reservoir brine.....	59
Figure 17. Effect of polyelectrolyte on equilibrium adsorption of surfactant on Brea Sandstone at reservoir brine. ....	60
Figure 18. Effect of surfactant/PSS addition techniques on equilibrium adsorption of surfactant on Brea Sandstone in reservoir brine. PSS concentration is 0.4 wt. % and is based on the amount of sand. ....	62
Figure 19. Dynamic surfactant adsorption in Brea sandstone packed bed at reservoir brine.....	63
Figure 20. Dynamic surfactant adsorption in Ottawa sand packed bed at reservoir brine .....	64
Figure 21. Effect of 70 KDa PSS on dynamic surfactant adsorption in Brea sandstone packed bed at reservoir brine. PSS and surfactant were injected sequentially.....	66
Figure 22. Effect of PSS/surfactant addition techniques on dynamic adsorption of surfactant and 70 KDa PSS in Brea sandstone packed bed at reservoir temperature.....	67
Figure 23. Sand pack studies conducted in (A) Ottawa sand and (B) Brea sandstone packed beds at the reservoir conditions (52° C) without polyelectrolyte. Surfactant injection protocol: 1 PV, 0.75 wt. % .....	68

Figure 24. Sand pack studies in the presence of PSSs (1 PV, 0.4 wt. %) and Surfactant (1 PV, 0.75 wt. %) in Brea sandstone packed beds. Studies performed with reservoir brine at reservoir temperature of 52° C ..... 69

Figure 25. Effect of 70 KDa PSS (1 PV, 0.4 wt. %) on oil mobilization in Brea sandstone packed bed at reservoir condition (52° C). Surfactant injection protocol: 1 PV, 0.75 wt. % ..... 70

Figure 26. Effect of PSS (70 KDa) concentration on oil recovery from Brea sandstone packed beds at reservoir condition (52° C). Surfactant injection protocol: 1 PV, 0.75 wt. % ..... 71

## Abstract

Developing a surfactant formulation for reservoir having high salinity/total dissolved solids (TDS) brine is a challenging task because surfactant not only phase separate or precipitate but also show high adsorption on reservoir rocks under such condition. These issues pose major threat on technological and economic viability of surfactant based chemical enhanced oil recovery (cEOR) technique. Therefore, this study attempts to overcome such challenges by investigating the feasibility of an alcohol free binary mixtures of sodium alkyl alkoxy sulfate surfactants and a sodium alkyl ethoxy sulfate surfactant for reservoir brine having a TDS of 301,710 mg/l with total hardness of 12,973 mg/l. The optimized surfactant formulations show excellent aqueous phase stability, produce an ultra-low-interfacial tension (IFT) of 0.004 mN/m, and give fast coalescence rates of less than 30 minutes at reservoir conditions. Accuracy of the hydrophilic lipophilic deviation (HLD) method in predicting the ratio between two surfactants to give optimal Type III microemulsion is also studied. Results show that correct determination of surfactant's head constant,  $K$ , and temperature constant,  $\alpha_T$ , determines the accuracy of the HLD method.

This study also demonstrates the field feasibility of the proposed surfactant formulation. Sand pack studies are performed in laboratory in order to optimize surfactant-only slug for field test. Single well tracer tests (SWTTs) are conducted before and after surfactant injection to assess the oil mobilization efficiency of laboratory optimized formulation at the field. Numerical simulation method is further applied to interpret field data. The results show approximately 73% reduction of residual oil saturation ( $S_{or}$ ) demonstrating the efficacy of lab optimized surfactant-only flood system in ultra-high TDS reservoir.

Furthermore, this work investigates the efficacy of polyelectrolyte, polystyrene sulfonate (PSS), as a sacrificial agent for lowering surfactant adsorption at reservoir conditions. Four different molecular weight PSSs are evaluated through equilibrium and dynamic adsorption studies carried out on Brea sandstone and Ottawa sand. Results show significant reduction in surfactant adsorption after PSSs addition. Moreover, the sand pack studies are conducted to evaluate the effect of PSS minimized surfactant adsorption on oil mobilization/recovery. Results indicate improved oil recovery in the presence of PSS suggesting its potential future as sacrificial agent in cEOR.

**Keywords** – Chemical enhanced oil recovery, Microemulsions, High total dissolved solids, Extended surfactants, Surfactant precipitation, Coalescence rate, Interfacial tension, Hydrophilic lipophilic deviation concept, Characteristic curvature, Single well tracer test, Equilibrium surfactant adsorption, Dynamic surfactant adsorption, Sacrificial agents, Polystyrene sulfonates, Sand pack study

## CHAPTER 1: Introduction

During oil production from a reservoir, the primary method, using natural pressure of the reservoir, and the secondary method, water flooding, together extract approximately 30 to 35 % of original oil in place from the reservoir<sup>1-2</sup>. The remaining oil stays trapped in the pores of reservoir rocks primarily due to capillary forces<sup>3-5</sup>. In surfactant-based chemical enhanced oil recovery (cEOR) techniques, this trapped oil can be unlocked by injecting surfactant solution into the reservoir. Surfactant being a dual polarity molecule, water-like and oil-like, partitions itself at the oil-water interface, decreases interfacial tension (IFT), and can increase capillary numbers enough to overcome capillary forces, which allows pore-locked oil to flow<sup>6-9</sup>. However, surfactant behaves differently at the different reservoir conditions and since each reservoir is characterized by its own oil type, brine salinity, rock type, and temperature, it is required to tailor cEOR surfactant formulation at the reservoir conditions<sup>10-11</sup>.

One of the main criteria of cEOR surfactant formulations is to exhibit a homogeneous, clear, single phase aqueous solution at the reservoir conditions<sup>12-13</sup>. However, under high salinity/TDS (total dissolved solids) reservoir brine environment, surfactant tends to precipitate or phase separate<sup>14-16</sup>. This becomes challenging for companies that want to make use of produced water in onshore cEOR projects or the available water sources such as sea water in offshore opportunities<sup>17</sup>. The alternative is to use fresh water, which may not always be available, or install brine-softening facilities, which may increase the total capital cost of the project making it less attractive for industries. In addition, loss of anionic surfactant on reservoir rocks due to adsorption is also found to be severe in high TDS brine<sup>18-19</sup>. The reservoir-injected surfactant slug, before reaching to the targeted oil zone, gets adsorbed onto the rocks or soil surfaces.



Alkali, which is being traditionally used to minimize adsorption of anionic surfactant, also precipitates and become ineffective at high TDS environment<sup>20-21</sup>. In such scenarios, a high amount of surfactant needs to be injected to satisfy the adsorption, which may not be economically feasible.

Moreover, screening high performance surfactants for cEOR is a challenging task. The established method for such application is the traditional trial and error surfactant phase behavior studies<sup>12</sup>. Even though this method is proven to be effective, the prolonged time (up to 6 months in some cases) it takes to develop a surfactant formulation makes such method very time consuming and inefficient. Recently several authors have proposed the quantitative structure-property relationship (QSPR) method for selecting cEOR surfactants by relating surfactant structure to their optimal salinities<sup>22-23</sup>. However, such a model has its own limitations: First, it does not take into account of reservoir properties such as brine salinity, oil type, and temperature; second, most of the commercially available surfactants are mixtures of homologues and exact composition/structure of these surfactant may not be available.

Therefore, this study attempts to overcome the above mentioned challenges by setting the following objectives:

- To study the performance of an alcohol free binary mixture of sodium alkyl alkoxy sulfates (extended surfactants) and sodium alkyl ethoxy sulfates (SAES) for a reservoir brine that has TDS of 301,710 mg/l with total hardness ( $\text{Ca}^{2+}$  and  $\text{Mg}^{2+}$ ) of 12,973mg/l. This is the highest TDS brine that has ever been addressed in the cEOR literature. Additionally, both extended and SAES surfactants are known to show excellent phase stability at high salinity conditions because of

their added polar groups such as propylene oxides (POs) and/ or ethylene oxides (POs)<sup>11</sup>.

- To demonstrate the viability of the hydrophilic lipophilic deviation (HLD) method as a surfactant pre-screening tool for cEOR. The HLD method is derived based on thermodynamic conditions and takes into account multiple reservoir properties<sup>24</sup>.
- To investigate the field feasibility of a laboratory-optimized surfactant formulation. Single well tracer tests<sup>25</sup> (SWTT) are carried out before and after surfactant injection to assess the oil displacement efficiency of the designed formulation.
- To test the effectiveness of negatively charged polyelectrolyte, polystyrene sulfonates (PSSs), in minimizing adsorption of anionic surfactant on Brea sandstone and Ottawa sand from high TDS brine. Polyelectrolytes can alter surface charge when adsorbed on oppositely charged surfaces<sup>26-27</sup>, such as clay surfaces.

The following three chapters discuss the results of this study. These chapters have either been submitted or will be submitted for publication in peer-review journals, and are presented here as word for word replication of their journal submitted forms. The topics of these chapters and the journals where these chapters are submitted or will be submitted are listed below:

- **Chapter 2:** “Design of an Optimal Middle Phase Microemulsion for Ultra High Saline Brine using Hydrophilic Lipophilic Deviation (HLD)

Method”. Submitted to “*Colloid and Surfaces A: Physicochemical and Engineering Aspects*”

- **Chapter 3:** Single Well Field Feasibility of Surfactant-Only Flooding in Extreme Saline Brine Reservoir. Will be submitted to “*Journal of Petroleum Science and Engineering*”
- **Chapter 4:** “Improved Oil Recovery by Reducing Surfactant Adsorption with Polyelectrolyte in High Saline Brine”. Will be submitted to “*Colloid and Surfaces A: Physicochemical and Engineering Aspects*”

## **CHAPTER 2: Design of an Optimal Middle Phase Microemulsion for Ultra High Saline Brine using Hydrophilic Lipophilic Deviation (HLD)**

### **Method**

#### **Introduction**

The importance of the middle phase microemulsion and its relation to ultra-low interfacial tension and chemical enhanced oil recovery (cEOR) is well understood<sup>28-29</sup>. Many researchers have extensively studied this area and have developed surfactants that can produce this type of microemulsion at different reservoir conditions<sup>17, 30</sup>. However, developing a surfactant formulation for sandstone reservoirs containing high total dissolved solids (TDS) brine (>200,000 ppm) is a challenging task. Shown in Figure 1 is the effect of high TDS on homogeneous single phase surfactant solution. The presence of monovalent and divalent cations, such as  $\text{Na}^+$ ,  $\text{K}^+$ ,  $\text{Ca}^{++}$ , and  $\text{Mg}^{++}$ , in the reservoir brine creates an unsuitable environment for the anionic surfactant by inducing surfactant precipitation or a two phase aqueous micellar solution<sup>14-15</sup>. Surfactant precipitation is the most common problem encountered at high TDS conditions. The counter-ions present in the aqueous solution may result in surfactant precipitation<sup>31</sup>. This situation can be exacerbated in the presence of a high concentration of divalent cations making it completely ineffective for cEOR application. The salting out of micelles or the formation of two phase aqueous micellar solution having both micelle rich and micelle poor phases can also be encountered at high salinity conditions<sup>32</sup>. Even though, at such condition, the surfactants are soluble in brine, it is highly undesirable for cEOR as it increases the IFT of the oil-water interface.

In recent years, surfactant formulations for high TDS brine are gaining popularity among industries because of growing onshore and offshore cEOR opportunities<sup>17</sup>. Industries

prefer to use the produced reservoir brine or available water sources (for example, seawater in offshore) for cEOR technique. However, surfactants cannot survive high TDS of the produced reservoir brine or sea water and thus requires brine softening facility. This increases the overall project cost making cEOR projects less attractive for industries. There is, therefore, a need for an innovation of surfactant formulation for high TDS brine condition.

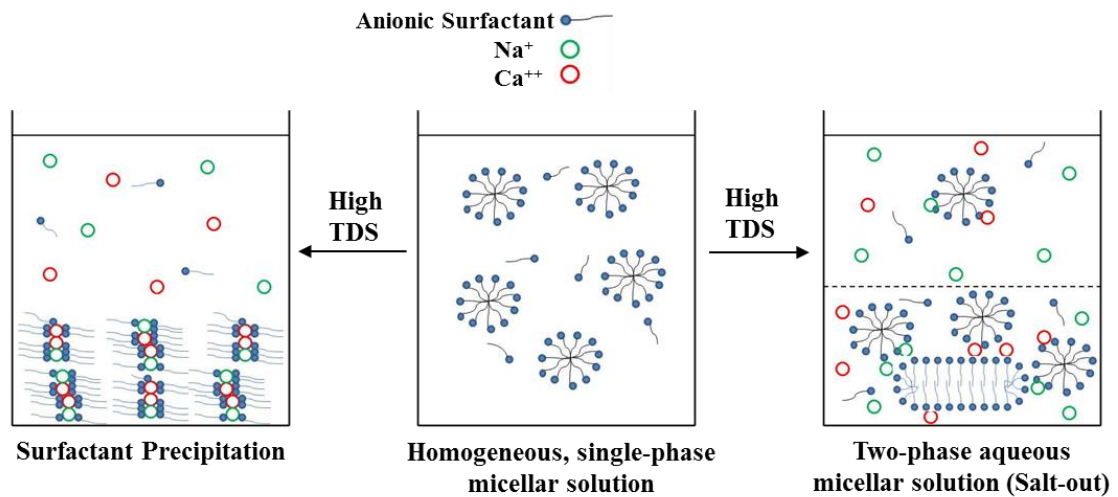


**Figure 1.** Effect of High TDS on homogeneous single phase micellar solution

It is well known that the sodium alkyl alkoxy sulfate surfactants, also known as extended surfactants, are suitable for high salinity brines<sup>11, 17, 33</sup>. By definition, extended surfactants have polypropylene oxides (POs) or a mixture of polyethylene oxides (EOs) and polypropylene oxides (POs) inserted between the hydrophilic heads and lipophilic tails<sup>34</sup>. According to Winsor's R ratio<sup>35</sup>, the best way to generate an optimal middle phase microemulsion, Type III, having equal amount of oil and water solubilized in the middle phase is to equally enhance surfactant-oil and surfactant-water interactions. These two interactions can be enhanced by making the surfactant's head group more hydrophilic and

tail group more hydrophobic. However, there is a possibility a conventional surfactant loses water solubility because of increased tail group hydrophobicity<sup>29</sup> and is not desirable for cEOR application<sup>11</sup>. In contrast, extended surfactants can maintain their stronger interaction with both water and oil phase while generating ultra-low IFT and without losing water solubility due to the presence of polar groups in the EOs and POs.<sup>11</sup> One of the drawbacks of extended surfactant is the hydrolysis of sulfur-to-oxygen (S-O) bond, which is present between its sulfate head group and alkoxy chain, above 60 °C<sup>36</sup>. Therefore, surfactants having sulfonate or carboxylate head groups are suggested for reservoirs with higher temperature conditions<sup>37</sup>. Another class of surfactant, that is sodium alkyl ethoxy sulfate<sup>38</sup>, is also reported to show promising results in high salinity brines. This class of surfactant is usually used as a co-surfactant in a surfactant mixture to enhance the overall hardness tolerance of surfactant mixture. Some authors also report the use of co-solvents such as short chain alcohols (sec-butanol and iso-propanol) to increase the solubility of surfactant in high salinity brine<sup>13,39</sup>. However, alcohols that are mostly used for eliminating gels/ liquid crystal formation in surfactant systems can adsorb together with the surfactant at the oil-water interface. In such cases, oil solubilization ability of the surfactant systems decreases and IFT increases which is undesirable for cEOR application<sup>40</sup>. Therefore, a careful consideration should be given in selecting surfactants and ingredients with the correct structure as this plays an important role in developing surfactant formulation for any cEOR process.

Most of the suggested formulations for high salinity brines are developed either for brines up to 21 wt % NaCl without hardness<sup>38</sup> or brines containing hardness up to 8,500 mg/l with a total TDS of 165,000 mg/l<sup>41</sup>. In this work, surfactant formulations for reservoir

brine having total TDS of over 300,000 mg/l with the total hardness of about 13,000 mg/l are reported. To date, this is the highest TDS brine that has ever been addressed. The alcohol free binary mixtures of extended surfactants and sodium alkyl ethoxylate surfactant (sodium laureth sulfate) with three EOs are evaluated through phase behavior studies, IFT measurements, and sand-pack tests at reservoir conditions. Moreover, the concept of hydrophilic lipophilic deviation (HLD) equation is used as the pre-screening tool for the purposed surfactant systems.

#### *Hydrophilic Lipophilic Deviation (HLD) Concept*

Salager *et al.*<sup>24</sup> first proposed the HLD concept as the thermodynamically derived correlation to describe microemulsion systems at the formulation conditions. Although, there are other correlations such as Winsor R ratio and HLB equation<sup>42</sup> to describe emulsion and microemulsion systems as well as the overall hydrophilic-lipophilic attraction of the surfactants, the practical applications of such correlations are still limited. For example, the parameters of Winsor R ratio are almost impossible to estimate, whereas the HLB concept has its own limitations of not taking into account of both equilibrium and formulation conditions. The HLD equation closes this gap by overcoming the limitations of both the Winsor R ratio and HLB equation. The negative, positive and zero values of HLD represents Type I, II and III microemulsion systems, respectively. There are two forms of the HLD equation, one form of the HLD equation is for ionic surfactants and the other form of the HLD equation is for nonionic surfactants<sup>24</sup>. Since the surfactants that are used in this research are anionic, the HLD equation is written as:

$$HLD = Cc + \ln(S) - K(EACN) - f(A) - \alpha_T(\Delta T) \quad (\text{Equation 1})$$

where  $C_c$  determines the hydrophobicity of a surfactant,  $S$  is the salinity of the aqueous phase in grams of NaCl per 100 ml. of solution,  $K$  is the constant whose value depends on surfactant head group and its hydrophilicity, EACN is the equivalent alkane carbon number of the oil used,  $f(A)$  is the alcohol constant,  $\alpha_T$  is a temperature constant, and  $\Delta T$  is the difference between formulation temperature,  $T$ , and the reference temperature,  $T_{ref}$ .  $T_{ref} = 25^\circ\text{C}$ .

Some researchers have reported that a change in system pressure results in changes to the optimal salinities<sup>43</sup> and have incorporated pressure correction factor in the HLD equation<sup>44</sup>. However, such an effect is found to be extremely small especially if the formulation condition is not very far, a few hundred bars, from atmospheric. Therefore the pressure term is neglected for this work.

At optimal condition, HLD is equal to zero and the salinity ' $S$ ' represents the optimal salinity ' $S^*$ '. Assuming  $T = T_{ref} = 25^\circ\text{C}$ , and if no alcohol is used i.e.  $f(A) = 0$ , the HLD equation can be rewritten as:

$$\ln S^* = K(EACN) - C_c \quad (\text{Equation 2})$$

If two or more different oil phases are used to determine the optimal salinities of a single surfactant system, the slope of the plot ( $\ln S^*$  vs EACN) is the  $K$ -value and the intercept is the  $C_c$  of that surfactant.

Surfactants with a long straight tail are known to form viscous microemulsions, gels or liquid crystals with various oil phases even at the optimal condition. In this situation, the equilibration time can last up to three to four weeks and in some cases it becomes very challenging to observe the actual middle phase microemulsions, making it extremely difficult to evaluate the HLD parameters. To overcome this, a linear surfactant mixing



rule proposed by Acosta *et al.*<sup>45</sup> is adapted to evaluate the parameters of the HLD equations. Sodium di-hexyl sulfosuccinate, AMA, is used as the reference surfactant. AMA is known to form translucent middle phase microemulsions with various oils, and when AMA is mixed with the surfactant of interest, visually translucent middle phases may form which makes it easier to estimate the HLD parameters of the surfactant of interest. Thus, Equation 2 can be conveniently written in the form of linear mixing rules as:

$$\ln S_{mix}^* = K_{mix}(EACN) - Cc_{mix} \quad (\text{Equation 3})$$

$$\text{Where } \ln S_{mix}^* = \sum x_i \ln S_i^* \quad (\text{Equation 4})$$

$$K_{mix} = \sum x_i K_i \quad (\text{Equation 5})$$

$$Cc_{mix} = \sum x_i Cc_i \quad (\text{Equation 6})$$

Where ‘i’ represents the surfactant i in the mixture and ‘x<sub>i</sub>’ is the mole fraction of the surfactant i. For mixtures of binary surfactants (1 and 2) and at x<sub>2</sub> = 1 - x<sub>1</sub>, Equation 4 is simplified and can be written as:

$$\ln S_{mix}^* = \{(Cc_1 - Cc_2) + (K_2 - K_1)(EACN)\}x_2 + \ln S_1^* \quad (\text{Equation 7})$$

The plot of  $\ln S_{mix}^*$  vs. x<sub>2</sub> gives a straight line with slope and intercept as follows:

$$\text{slope} = \{(Cc_1 - Cc_2) + (K_2 - K_1)(EACN)\} \quad (\text{Equation 8})$$

$$\text{intercept} = \ln S_1^* = K_1(EACN) - Cc_1 \quad (\text{Equation 9})$$

The HLD parameters (Cc, K, and  $\alpha_T$ ) of the reference surfactant, AMA, are reported in the literature<sup>45</sup>. By knowing the parameter ‘K<sub>2</sub>’ of the surfactant of interest, its Cc-value is calculated using Equation 8.

Even though the HLD equation is based on equilibrium conditions and its parameters are relatively easy to estimate, to date very limited work has been done to design a surfactant

formulation for cEOR applications by using the HLD concept. Recently, Tarahan *et al.*<sup>46</sup> observe that the surfactants of the extended surfactant family having similar  $C_c$ -values give comparable phase behavior and coreflood results. However, depending on the surfactant family and structure, each surfactant behaves differently at different formulation conditions. Also most of the developed cEOR surfactant formulations incorporate binary or ternary blends of different class of surfactants. Therefore, in this work, besides the  $C_c$ -values, the surfactant temperature dependence parameter,  $\alpha_T$ , as well as the surfactant head dependent parameter, the  $K$ -value, of the HLD equation are taken into account for designing high TDS surfactant formulations at the targeted reservoir conditions. The HLD equation is used: to estimate the required  $C_c$  at which the optimal Type III microemulsion is formed at the reservoir condition, to predict the desired ratio of surfactant/co-surfactant by using Equation 6 in order to match similar  $C_c$ -value as calculated by Equation 1, and to eventually compare the accuracy of these correlations with the experimental results obtained independently through phase behavior studies and IFT measurements.

## **Experimental**

### *Materials*

The extended surfactants used in this study were kindly provided by Sasol North America Inc., Lake Charles, LA. The co-surfactant i.e., sodium laureth sulfate, trade name Steol Cs460, was purchased from Stepan Chemical Inc. sodium dihexyl sulfosuccinate (Aerosol-MA, AMA), sodium chloride (>99%), toluene (>99.8%), limonene, hexane, octane (>99.5%), decane (>98%) were purchased from Sigma Aldrich. All the surfactants and oils were used as received. Detailed information of individual surfactants can be found in Table 1.

**Table 1.** Surfactant Properties

Surfactants	Commercial name/ Trade name	# of EOs	# of POs	Alkyl C#	MW (g/mol)	Active wt. %
C <sub>8</sub> -(PO) <sub>4</sub> -(EO) <sub>1</sub> -SO <sub>4</sub> Na	-	1	4	8	507	32.3
C <sub>8</sub> -(PO) <sub>4</sub> -SO <sub>4</sub> Na	-	-	4	8	466	33
C <sub>10</sub> -(PO) <sub>4</sub> -(EO) <sub>1</sub> -SO <sub>4</sub> Na	-	1	4	10	538	32.2
C <sub>10</sub> -(PO) <sub>4</sub> -SO <sub>4</sub> Na	-	-	4	10	493	32.5
C <sub>16</sub> H <sub>29</sub> O <sub>4</sub> -SO <sub>3</sub> Na	Sodium dihexyl sulfosuccinate (AMA)	-	-	6 (Twin tail)	388.45	80
C <sub>12</sub> -SO <sub>4</sub> Na	Sodium dodecyl sulfate (SDS)	-	-	12	288	≥99
C <sub>12</sub> -(EO) <sub>3</sub> -SO <sub>4</sub> Na	Sodium laureth sulfate (Steol Cs460)	3	-	12	441	60

**Table 2.** Reservoir Brine Analysis. Analysis Conducted by Red River Laboratory, Oklahoma City, OK

Components	Concentration (mg/l)
Sodium	51675
Potassium	1076
Magnesium	2868
Calcium	10105
Iron	10.3
Sulfate	341
Chlorine	235634
Total hardness (Ca <sup>++</sup> and Mg <sup>++</sup> )	<b>12973</b>
Total dissolved solids	<b>301710</b>

**Table 3.** Characteristic of the crude oil. Analysis conducted by Harris Testing Laboratory, Houston, TX

Density (g/ml)	Viscosity (52°C) cP	Acid number (mg of KOH/g of sample)
0.82	4.5	0.44

The reservoir brine and crude samples were collected from the targeted War Party site which is located near Guymon, Oklahoma. The received brine samples were first filtered using the one micron filter paper. A complete analysis of the brine is listed in Table 2 and the characteristics of the crude oil can be found in Table 3. The F-95 grade Ottawa sand (60-170 mesh size) that was used in the one-dimensional sand pack experiments was provided by U.S. Silica, Mill Creek, OK and was used as received.

#### *Microemulsion Phase Study*

An initial salinity scan was conducted to determine both Cc-values and K-values of the chosen surfactants. A total of 5 ml oil phase and 5 ml of aqueous phase containing a mixture of surfactants were added into a vial, hand-shaken once a day for two sequential days and were allowed to equilibrate for at least one week period at 25°C. The relative amount of oil, water, and microemulsion of equilibrated samples in the vial were then quantified. The system with equal amount of oil and water solubilized in the middle phase microemulsions is referred as the optimal formulation and used to determine the ‘optimal salinity,’ S\* for each ratio of surfactants. All the studies were performed keeping the total surfactant concentration of the water phase constant at 0.10 M.

Microemulsions phase studies for the site-specific reservoir crude oil and brine were conducted by varying the ratios of surfactants/co-surfactants in the binary mixture. Similarly, 5 ml of crude oil and 5 ml of aqueous phase were placed into the vial, hand-shaken once a day for two days and stored inside an oven (maintained at reservoir temperature of 52°C) for at least one week for equilibration. For verification, the IFTs of equilibrated samples were also measured and the formulation generating the lowest IFT-value is considered the optimal microemulsion system.

### *Stability Study of Surfactant Solution*

The phase stability tests were conducted to determine the solubility and possible phase separation of the test surfactants in reservoir brine at reservoir temperature. The 5 mL samples of the surfactant solution were kept inside the oven (52 °C) and were periodically monitored once every 15 days up to 120 days for any surfactant precipitation and/or phase separation.

### *Equilibrium IFT Measurement*

The IFT measurements of equilibrated samples were conducted using a spinning drop tensiometer (M6500 Grace Instrument, Houston, Texas). The samples, approximately 1-5  $\mu$ L of excess oil phase, were collected from the top portion of equilibrated sample vials and was injected carefully into the spinning capillary tube that was pre-filled with excess aqueous phase collected from the bottom of the same vial. The data were recorded every 5 minutes until the last two readings stabilized to within  $\pm 3\%$ .

### *One-Dimensional Sand-Pack Test*

The F-95-grade Ottawa sand was used for the sand-pack tests. A glass chromatography column that is 6 inches long and 1 inch in diameter was first filled with approximately 10 mL of reservoir brine for wet-packing procedure. Several grams of sand was added from the top of the column until the added sand particles reached slightly below the brine level. A spatula is used to swirl sand around to facilitate uniform packing. Once evenly distributed, additional brine and sand were repeatedly introduced until the glass column was fully packed with water-saturated sand. After fully saturating the column with brine, reservoir oil injection was initiated by inverting the column position and injecting oil from the outlet of the column to ensure the uniform oil saturation. Once the water cut of

the effluent reached less than 1%, the oil injection was switched back for the brine injection. During brine injection, the column was inverted again and the brine was injected from the bottom. The waterflood was carried out until the oil cut of the effluent is less than 1%. The pre-determined surfactant-only flooding protocol of 1 pore volume (PV) of surfactant solution was then carried out and was followed by 3 to 4 PVs of post-chemical brine. The injection rate of each fluid was maintained at 0.3 ml/min, unless noted otherwise.

## Results and Discussion

### *Determination of K and Cc-values*

Depending on the structures of the surfactant head group, the K values of anionic surfactants are found to be in the range of 0.004 to 0.17<sup>24, 45, 47-49</sup>. Yet, for simplicity, Acosta *et al.* recommends to assume the K-value of anionic surfactants as 0.17 for determining other parameters of HLD equation<sup>45</sup>. However, based on our observation, selecting the correct K-value gives more precise results. Thus, if possible, it is recommended to determine the K-value for each individual surfactant along with the other parameters of HLD equation, for better accuracy.

**Table 4.** Effect of surfactant structure on optimal salinity; S\* is in g of NaCl/100 ml solution and total surfactant concentration is 0.1M

Surfactants	Hexane S*(±0.3)	Octane S*(±0.3)	Decane S*(±0.3)
C <sub>8</sub> -(PO) <sub>4</sub> -(EO) <sub>1</sub> -SO <sub>4</sub> Na	16.2	18.3	20
C <sub>8</sub> -(PO) <sub>4</sub> -SO <sub>4</sub> Na	16.5	18.7	20.5
C <sub>10</sub> -(PO) <sub>4</sub> -(EO) <sub>1</sub> -SO <sub>4</sub> Na	13.5	15.6	17.5
C <sub>10</sub> -(PO) <sub>4</sub> -SO <sub>4</sub> Na	12.9	15.1	17

Based on Equation 2, the ability of a test surfactant to form a middle phase with various oils (i.e., different EACNs) is crucial for the determination of its K-value. In general, the selected surfactants used in this study are able to form the middle phase microemulsion with hexane, octane, and decane. The resulted salt concentration at which an equal amount of water and oil are solubilized in the middle phase is the optimal salinity ( $S^*$ ) for that particular EACN of oil. The optimal salinities of individual surfactants tested with these oils are summarized in Table 4. In Table 4, it is observed that the optimal salinity of each surfactant increases with increasing EACN of the oil. This phenomenon can be best understood with help of Winsor R concept<sup>35</sup> defined as the ratio of net surfactant-oil interactions,  $A_{co}$ , to the net surfactant-water interaction,  $A_{cw}$ . Increasing the EACN of the oil decreases the  $A_{co}$  and to balance this effect, the  $A_{cw}$  is decreased by adding salt. Salt reduces the  $A_{cw}$  by compressing the electrical double layer of the surfactant head group<sup>50</sup>. A similar concept of the salt effect can be applied to describe the effect of increase in carbon tail length of a surfactant in decreasing the optimal salinity. For example, as shown in Table 4, the optimal salinities of  $C_8-(PO)_4-SO_4Na$  are higher with any oil compared to that of  $C_{10}-(PO)_4-SO_4Na$ . In Table 4, the optimal salinities of  $C_8-(PO)_4-SO_4Na$  with all oils are higher compared to that of  $C_8-(PO)_4-(EO)_1-SO_4Na$ . The difference between these two surfactants is the presence of one extra EO group. One would expect that the presence of EO increases the  $A_{cw}$  and thereby increases the optimal salinity. However, the presence of up to 2 EO groups in an anionic surfactant decreases the optimal salinity<sup>51</sup>. The explanation given for this phenomenon is that at the oil-water interface, the methyl group of the corresponding EO encounters the hydrated environment and adding one EO doesn't increase the effective size of the head group and thereby

decreases the optimal salinity. Conversely, addition of more than two EOs is expected to increase the overall size of the surfactant head and thus increases the optimal salinity. Also observed in Table 4, the same phenomenon is not valid in the case of C<sub>10</sub>-(PO)<sub>4</sub>-SO<sub>4</sub>Na and C<sub>10</sub>-(PO)<sub>4</sub>-(EO)<sub>1</sub>-SO<sub>4</sub>Na where optimal salinities of C<sub>10</sub>-(PO)<sub>4</sub>-(EO)<sub>1</sub>-SO<sub>4</sub>Na are higher compared to that of C<sub>10</sub>-(PO)<sub>4</sub>-SO<sub>4</sub>Na. This behavior can be explained due to the fact that there might be a distribution in the number of EOs and POs as well as a commercial mixture of alkyl chain lengths in the alcohols which might have affected the results.

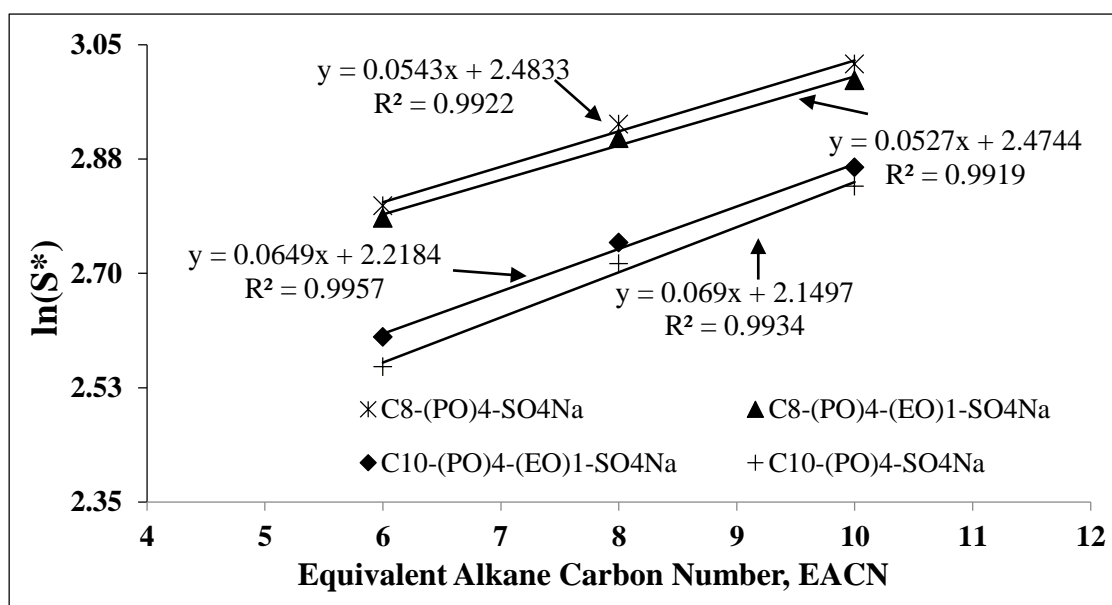


**Figure 2.** Plot of  $\ln(S^*)$  Vs EACN to determine the K and C<sub>c</sub> of the extended surfactants. The optimal salinities determined for the extended surfactants with three different alkanes were used to construct a graph of  $\ln S^*$  against EACN, which is shown in Figure 2. According to Equation 2, the slope of the line fit to these data is the K-value and the y-intercept is the C<sub>c</sub>-value. Figure 2 shows the R<sup>2</sup> value of each fitting is above 0.99 suggesting the linear fitting is in very good agreement with the trend in data. The calculated K-values and C<sub>c</sub>-values of the extended surfactants are listed in Table 5. Table



5 shows the K-values of the extended surfactant to be in the range of 0.05 to 0.07. Hammond *et al.* report the K-values for the extended surfactant, C<sub>12</sub>-(PO)<sub>4</sub>-SO<sub>4</sub>Na family, to be in the range of 0.04 to 0.06, which is in good agreement with the K-values that are reported in this paper. Other authors have reported the K-value of the extended surfactant family to be in the range of 0.07 to 0.12<sup>49</sup>. However, the average K-value, 0.06 ± 0.007 determined in this work from slope of the fitted lines shown in Figure 2 is used for extended surfactants.

**Table 5.** Experimentally obtained K-values and Cc-values of extended and conventional surfactants unless otherwise noted. Cc\* is the Cc-value calculated by using group contribution correlation

Surfactants	K	Cc	Cc*
C <sub>8</sub> -(PO) <sub>4</sub> -(EO) <sub>1</sub> -SO <sub>4</sub> Na	0.053	-2.47	-
C <sub>8</sub> -(PO) <sub>4</sub> -SO <sub>4</sub> Na	0.054	-2.48	-2.38
C <sub>10</sub> -(PO) <sub>4</sub> -(EO) <sub>1</sub> -SO <sub>4</sub> Na	0.065	-2.22	-
C <sub>10</sub> -(PO) <sub>4</sub> -SO <sub>4</sub> Na	0.069	-2.15	-2.18
C <sub>12</sub> -SO <sub>4</sub> Na	0.1 <sup>48</sup>	-2.61	-
C <sub>12</sub> -(EO) <sub>3</sub> -SO <sub>4</sub> Na	0.06 <sup>47</sup>	-2.89	-

The Cc-value provides insight into the hydrophobicity of the surfactant<sup>47-48</sup>. Surfactants with negative Cc-values have a tendency to form a Type I microemulsion, whereas surfactants with positive Cc-values are more inclined to form a Type II microemulsion<sup>48</sup>. Shown in Table 5 are the K-values, Cc-values, and Cc\*- values determined for the surfactants that are studied in this work. The surfactants with the longer, C<sub>10</sub>, carbon chain have less negative Cc-values than surfactants with shorter, C<sub>8</sub>, carbon chains. The reason for the less negative Cc-values of the C<sub>10</sub> surfactants, relative to the C<sub>8</sub> surfactants, is due

to the increase in carbon chain length which increases the hydrophobicity of a surfactant. Table 5 also shows the addition of one EO to the extended surfactants doesn't have any significant effect on Cc-values. It is observed in Table 5 that both C<sub>8</sub>-(PO)<sub>4</sub>-SO<sub>4</sub>Na and C<sub>8</sub>-(PO)<sub>4</sub>-(EO)<sub>1</sub>-SO<sub>4</sub>Na exhibit similar Cc-values, -2.48 and -2.47 respectively, while the Cc of C<sub>10</sub>-(PO)<sub>4</sub>-SO<sub>4</sub>Na is -2.15 and is slightly more positive compared to -2.22 for C<sub>10</sub>-(PO)<sub>4</sub>-(EO)<sub>1</sub>-SO<sub>4</sub>Na. However, the difference in Cc-values of C<sub>10</sub>-(PO)<sub>4</sub>-SO<sub>4</sub>Na and C<sub>10</sub>-(PO)<sub>4</sub>-(EO)<sub>1</sub>-SO<sub>4</sub>Na is less than 1% and is acceptable given the error in measurements and the assumptions that has been made. This observation shows that the effect of EO on Cc-value of an extended surfactant is inconclusive as the addition of a single EO group does not affect the Cc significantly.

The Cc-values of extended surfactants calculated in this work can be compared with the predicted Cc-value that are obtained by using a group contribution model. Salager *et al.*<sup>52</sup> proposed such a model and later on, Hammond *et al.*<sup>48</sup> expanded the model to take into account the geometric shape of the surfactant tail, adding a contribution of surfactant tail branching to the model. It is unknown if the carbon tail structure of the tested extended surfactants is linear or branched, the carbon tail is assumed linear and the group contribution model is used to predict the Cc values marked as Cc\* in Table 5. The predicted Cc-values, -2.38 and -2.18 for C<sub>8</sub>-(PO)<sub>4</sub>-SO<sub>4</sub>Na and C<sub>10</sub>-(PO)<sub>4</sub>-SO<sub>4</sub>Na using the group contribution model are in good agreement with the experimental Cc-values, -2.48 and -2.15 of the same two surfactants studied in this work. The same model is not used for the extended surfactants having both EOs and POs since a reliable relationship between EO groups of the extended surfactant family and Cc has yet to be determined.

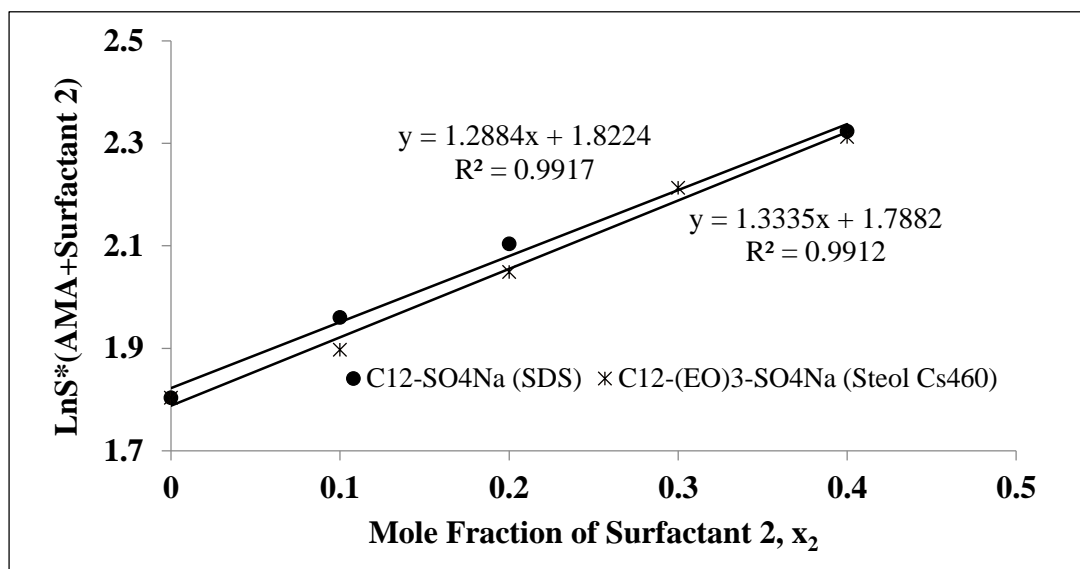


**Figure 3.** Effect of surfactant mixture (AMA and SDS or Steol Cs460) composition on overall salinity; Surfactant 2 is SDS or Steol Cs460. Oil phase is Limonene

Unlike the selected extended surfactants used in this work, the conventional surfactants such as  $C_{12}\text{-SO}_4\text{Na}$  (SDS) and  $C_{12}\text{-(EO)}_3\text{-SO}_4\text{Na}$  (Steol Cs 460) with 3 EOs were unable to form the middle phase microemulsion with these alkanes under similar conditions. Such behavior of SDS and Steol Cs460 is attributed to the increased surfactant tail-tail interaction at the oil water interface which leads to the formation of a gel instead of bi-continuous swollen micellar structure. Therefore, a surfactant mixing rule using limonene whose EACN is 5.7<sup>47</sup> is used as an oil phase to determine the  $C_c$ -values of both SDS and Steol Cs460. Figure 3 shows the graph of  $\ln(S^*)_{(\text{AMA} + \text{Surfactant 2})}$  vs mole fraction ( $x_2$ ) of surfactants whose  $C_c$ -values need to be determined. In Figure 3, it can be observed that the optimal salinities of SDS at any ratio with AMA are higher compared to that of Steol Cs460. The behavior of Steol Cs460 shows that the addition of up to three EOs decreases the optimal salinity which is slightly different compared to the data reported in the literature<sup>51</sup> i.e., addition of up to two EOs in a surfactant decreases the optimal salinity

and any further addition of EO increases the optimal salinity. Steol Cs460 is a commercial product with a distribution of EO's having an average of 3 EO's and this may have had an impact on the results relative to a surfactant without a distribution of EO's and all of the surfactant having exactly 3 EO's. In Figure 3, it is also observed that the  $R^2$  values of linear fitting are above 0.99 which confirms the validity of the linear assumption of surfactant mixing rule. Using Equation 8 and the slope that is obtained from Figure 3, the  $Cc_2$  values of both SDS and Steol Cs460 are determined and are listed in Table 5. In equation 8,  $Cc_1$  and  $K_1$  are the HLD parameters of a reference surfactant, AMA, whose values are -0.93 and 0.17 respectively<sup>45</sup>. The  $K_2$  parameter of Equation 8 is the K-value of SDS or Steol CS460. SDS is a commonly studied surfactant and its K-value is reported as 0.1 in the literature<sup>24, 45</sup>. No author has reported the K-value of  $C_{12}-(EO)_3-SO_4Na$  (Steol Cs460), and the reasoning behind this might be its inability to form a middle phase with various oils without the addition of a reference surfactant. However, the K-value of  $C_{12}-(EO)_2-SO_4Na$  (Steol Cs 230) is reported as 0.06<sup>47</sup>, and since its structure is very similar to that of Steol Cs460, it is assumed that both of these surfactants have similar K-values. The calculated Cc-value, -2.61, of SDS in this paper is in good agreement with values that are reported in the literature which range from -2.36 to -2.8<sup>45, 53</sup>. Witthayapanyanon *et al.*<sup>47</sup> have reported the Cc-value of Steol Cs 230 to be  $-2.96 \pm 0.25$ . This value is slightly lower compared to the Cc-value, -2.87, of Steol Cs460 that is determined in this study. In theory, because of one extra EO, Steol Cs460 should have a more negative Cc-value compared to that of Steol Cs230. Therefore, it is speculated that the both Steol Cs460 and Steol Cs230 being commercial mixtures with the distribution in EOs and alkyl chain length of alcohols might have resulted in such a discrepancy.

### *Temperature Dependence of Extended and Conventional Anionic Surfactants*

The temperature dependence,  $\alpha_T$ , of ionic surfactants is best understood using the HLD equation for ionic surfactants which is Equation 1. At the optimal formulation condition,  $HLD = 0$ , and when no alcohol is used,  $f(A) = 0$ , the Equation 1 can be rewritten as:

$$\ln(S^*) = K(EACN) - Cc + \alpha_T(\Delta T) \quad (\text{Equation 10})$$

According to Equation 10, the plot of  $\ln(S^*)$  vs  $\Delta T$  for a single surfactant system i.e.  $Cc$  and  $EACN$  are constant, shows that the optimal salinity of an ionic surfactant increases with increasing temperature. Such behavior of ionic surfactants can be explained due the fact the head group of an ionic surfactant becomes more hydrophilic at higher temperature which increases the optimal salinity and the solubility constant<sup>49</sup>. The temperature constant,  $\alpha_T$ , of ionic surfactants has been reported as  $0.01^\circ\text{C}^{-1}$ <sup>24, 48</sup>. In the case of extended surfactants, mixed views about their temperature dependence can be found. Some authors<sup>52</sup> have claimed that extended surfactants behave like mixtures of anionic and nonionic surfactants with increasing temperature. In another words, these systems do not show any significant temperature dependent behavior. This is because the extended surfactants contain ionic head groups and non-ionic polar groups, POs and EOs, in the same molecule, which nearly balances any temperature effect. Hammond *et al.*<sup>48</sup> found the optimal salinity of  $C_{12}-(PO)_4-SO_4Na$  decreases with the increase in temperature and has reported the  $\alpha_T$  value as  $-0.0059^\circ\text{C}^{-1}$ . Some authors also noticed the same behavior and have reported the  $\alpha_T$  values of extended surfactants to be in the range of  $-0.008$  to  $-0.012^\circ\text{C}^{-1}$ <sup>49</sup>. The  $\alpha_T$  value reported by the group of Hammond for extended surfactants is used in our calculations, since the number of PO's in the extended surfactants that are used in this study and by the group of Hammond are exactly the same.

Very limited studies have been done to identify the temperature dependence of sodium alkyl ethoxylate sulfate surfactants in microemulsions. Looking at the structure of alkyl ethoxylate sulfate surfactants, one would assume that, similar to PO groups of extended surfactants, the oxygen atoms of EO groups present in alkyl ethoxylate sulfate dehydrates at higher temperature and decreases the optimal salinity. However, Vasquez *et al.*<sup>49</sup> have mentioned the slope,  $\alpha_T$ , of the  $\ln S^*$  vs temperature plot for extended surfactant having both POs and EOs groups are higher compared to non-EO extended surfactants. This suggests that the decrease in optimal salinity with the increase in temperature is a function of POs not EOs. Skauge *et al.*<sup>43</sup> reported the temperature effect on optimal salinities of alkylaryl ethoxylate sulfonate having 4 EOs and report that the optimal salinities of such system increase with increasing temperature. Based on the available literature data, it is safe to assume that at higher temperature, the increases in hydrophilicity of the ionic head group is much larger compared to the dehydration of EO groups and thus the positive increase in  $\alpha_T$  of  $\ln S^*$  vs temperature plot is expected. Therefore, for similar reasons, the  $\alpha_T$  value of  $0.01^\circ\text{C}^{-1}$  is used for  $\text{C}_{12}\text{-(EO)}_3\text{-SO}_4\text{Na}$  (Steol Cs460) in this work.

#### *Prediction of Surfactant/Co-Surfactant Ratio*

The HLD predicts the Cc-value that is required to form an optimal Type III microemulsion at the reservoir conditions and is calculated by using Equation 1. Since the parameters, K and  $\alpha_T$ , of Equation 1 depend on the type of surfactant, the mole-average K and  $\alpha_T$  values are used. The HLD predicted Cc is shown in Table 6.

**Table 6.** Calculated required or predicted Cc to produce optimal Type III microemulsion of the site specific crude and brine at the reservoir conditions

TDS (S*)	Ave K	Ave $\alpha_T$	Temperature	EACN	Predicted Cc
30.17 g/100 ml	0.06	0.002 °C <sup>-1</sup>	52 °C	9.8	-2.76

**Table 7.** Predicted mole fraction (x) and weight fraction (y) of the binary mixtures to produce optimal type III microemulsions

Systems with Steol Cs460	Extended Surfactant (Primary Surfactant)		Steol Cs460 (Co-Surfactant)	
	x <sub>1</sub>	y <sub>1</sub>	x <sub>2</sub>	y <sub>2</sub>
C <sub>8</sub> -(PO) <sub>4</sub> -(EO) <sub>1</sub> -SO4Na	0.31	0.34	0.69	0.65
C <sub>8</sub> -(PO) <sub>4</sub> -SO4Na	0.32	0.31	0.68	0.69
C <sub>10</sub> -(PO) <sub>4</sub> -(EO) <sub>1</sub> -SO4Na	0.19	0.22	0.81	0.78
C <sub>10</sub> -(PO) <sub>4</sub> -SO4Na	0.17	0.19	0.83	0.81

Using the calculated Cc-values of the surfactants that are used in this study, the surfactant/co-surfactant ratio to form an optimal Type III microemulsion was predicted using Equation 7. The mole fraction of surfactants are varied until the Cc<sub>mix</sub> is similar to the HLD predicted Cc-value, -2.76. The predicted mole fractions and weight fractions of the binary mixtures are listed in Table 7. It is observed that the extended surfactant with the longer carbon chain length, C10, requires more Steol Cs460 to generate a Type III microemulsions compared to the shorter carbon chain length, C8. This trend can be explained due to the fact that increasing the number of carbon molecules in the tail makes the extended surfactant more hydrophobic and adding additional hydrophilic co-surfactant, Steol Cs460, balances such effects and keeps the system in a Type III microemulsion region.

*Phase Behavior Study and Surfactant Stability Test*

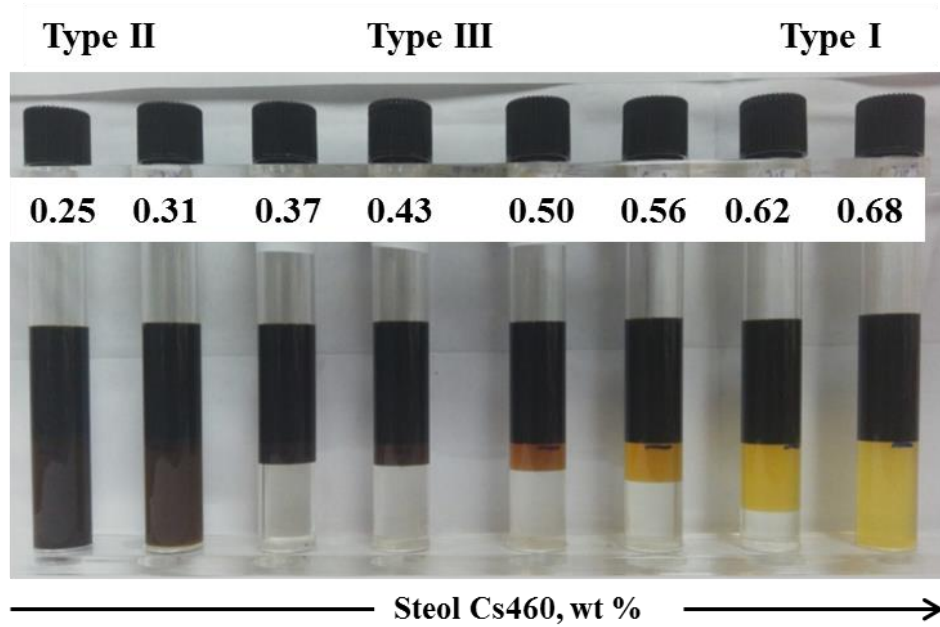


**Figure 4.** Phase behavior: Steol Cs460 scan for  $C_8-(PO)_4-(EO)_1-SO_4Na$  (0.25 wt. %) at the reservoir temperature ( $52^\circ C$ ) with crude oil

**Table 8.** Phase behavior studies, IFT measurement, and concentration of Steol Cs460 at optimal for each surfactant mixture. The concentration of extended surfactants at optimal is 0.25 wt %.

Systems with Steol Cs460	Aqueous Phase Stability	Coalescence Time, minutes	Optimal IFT, $\pm 5E-4$ mN/m	Steol Cs wt. % at Optimal
$C_8-(PO)_4-(EO)_1-SO_4Na$	Clear/single phase	< 25	8.68E-03	0.437
$C_8-(PO)_4-SO_4Na$	"	< 20	6.07E-03	0.375
$C_{10}-(PO)_4-(EO)_1-SO_4Na$	"	< 30	4.08E-03	0.667
$C_{10}-(PO)_4-SO_4Na$	"	<30	4.92E-03	0.687

To verify our claim above, phase behavior studies are conducted by holding the concentration of the extended surfactant constant at 0.25 wt % and varying the concentration of Steol Cs460 from the point where the surfactant mixture is predicted to form the optimal middle phase microemulsions as shown in Table 7. An example phase



behavior scan of  $C_8-(PO)_4-(EO)_1-SO_4Na$  and Steol Cs460 is shown in Figure 4. Table 8 gives the information of surfactant aqueous phase stability and the coalescence time of the region where middle phase microemulsions are formed. As noticed in the Table 8, all surfactant systems show a single, clear, and homogeneous aqueous phase indicating that surfactant precipitation or salting out is not present or observed. Additionally, the coalescence time is observed to be less than 30 minutes which is in the range for a robust surfactant formulation giving good oil recovery<sup>12, 54</sup>.

#### *IFT Measurements and Optimal Point*

The IFT measurement data of the surfactant mixtures as the function of Steol Cs460 concentration are shown in Figure 5. Focusing on Figure 5, the concentration of Steol Cs460 at which the minimum IFT value is observed is considered the optimal point for that specific system. At the optimal point, surfactants have an equal affinity for both oil and water phases and thus most of the surfactants migrate from the bulk oil and water phases into a separate middle phase containing equal volumes of oil and water; at these conditions a minimum IFT is achieved<sup>29, 55</sup> at the interface between the bulk oil and water phases. The IFT values and the Steol Cs460 concentration of surfactant mixtures at the optimal point are presented in Table 8. In addition to the ultralow IFT ( $<10^{-3}$  mN/m) nature of the optimal point as shown in Table 8, the coalescence time at the optimal region of each surfactant system are also observed to be less than 30 minutes. This behavior further verifies that the HLD predicted surfactant formulation satisfies the requirement of a robust surfactant formulation for a cEOR application<sup>7, 56</sup>. The sand pack study discussed below validates the designed formulation.

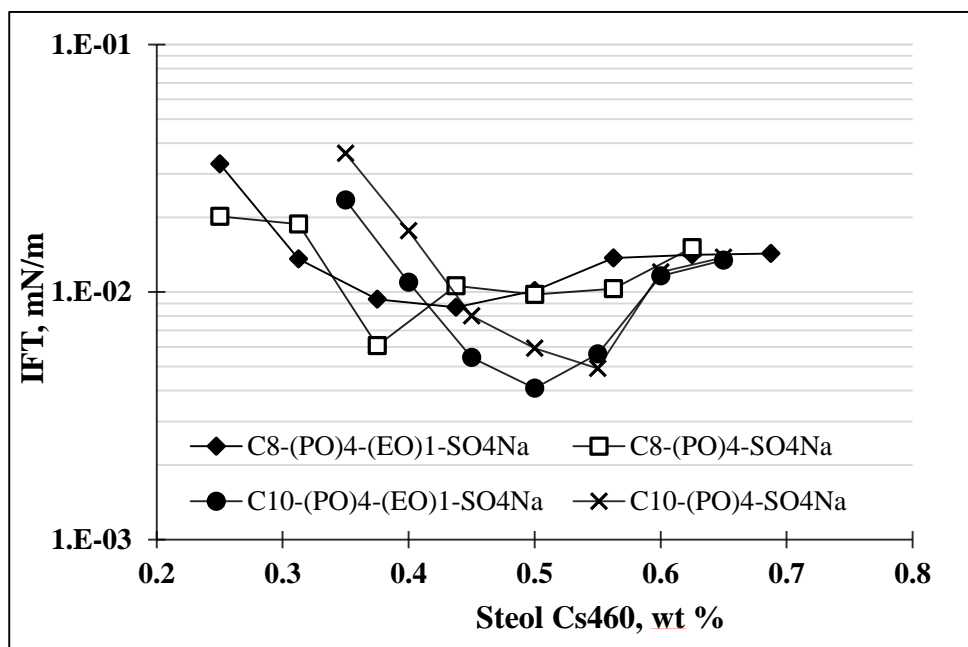


**Figure 5.** Equilibrium IFT measurements of the binary mixtures (extended surfactant, 0.25 wt. % + Steol Cs460) with the reservoir crude oil at 52°C

In general, surfactants with longer carbon tail length have stronger interactions with the oil phase and thus generate a lower IFT compared to the surfactant with the shorter carbon tail length<sup>28</sup>. Therefore, as shown in Figure 5 and also in Table 8, the optimal IFT values of extended surfactants with C<sub>10</sub> carbon chain length have lower IFT values than the ones with C<sub>8</sub> carbon chain length. Also shown in Figure 5 and Table 8, the amount of Steol Cs460 required at optimal point is lower for the extended surfactants with shorter carbon chain lengths, C<sub>8</sub>, compared to the ones with C<sub>10</sub> carbon chain length. Such a phenomenon can be understood with similar reasoning given for surfactants with longer carbon chain length having lower optimal salinities and less negative C<sub>c</sub>-values and vice-versa. In addition, as shown in Figure 5, the concentration of Steol Cs460 at optimal for C<sub>8</sub>-(PO)<sub>4</sub>-(EO)<sub>1</sub>-SO<sub>4</sub>Na system is almost 15% higher than that of the C<sub>8</sub>-(PO)<sub>4</sub>-SO<sub>4</sub>Na system. This observation further verifies that the addition of one EO decreases the optimal salinity which is also shown in Table 4. However, a similar conclusion cannot be drawn

in the case of C<sub>10</sub>-(PO)<sub>4</sub>-(EO)<sub>1</sub>-SO<sub>4</sub>Na and C<sub>10</sub>-(PO)<sub>4</sub>-SO<sub>4</sub>Na, and might be due to these compounds being commercial mixtures of homologues.

*Accuracy of the HLD Equation*

**Table 9.** Accuracy validation of the HLD equation

<b>Extended surfactant with</b>	<b>Predicted</b>	<b>Experimental</b>	<b>HLD Error</b>
<b>Steol Cs460</b>	<b>Cc<sub>mix</sub></b>	<b>Cc<sub>mix</sub></b>	<b>[(Cc<sub>Exp.</sub> - Cc<sub>Pred.</sub>)/Cc<sub>Exp.</sub>]<math>\times</math>100%</b>
C <sub>8</sub> -(PO) <sub>4</sub> -(EO) <sub>1</sub> -SO <sub>4</sub> Na	-2.76	-2.75	0.36
C <sub>8</sub> -(PO) <sub>4</sub> -SO <sub>4</sub> Na	-2.76	-2.73	1.1
C <sub>10</sub> -(PO) <sub>4</sub> -(EO) <sub>1</sub> -SO <sub>4</sub> Na	-2.76	-2.73	1.1
C <sub>10</sub> -(PO) <sub>4</sub> -SO <sub>4</sub> Na	-2.76	-2.71	1.85

The accuracy of the HLD equation is evaluated by comparing the experimentally observed Cc<sub>mix</sub>-values of each surfactant system with the HLD predicted Cc<sub>mix</sub>-value, -2.76, shown in Table 6. The experimental Cc<sub>mix</sub>-values are calculated using Equation 6, where the ‘X<sub>i</sub>’ term represents the experimentally determined mixture mole fractions of Steol Cs460 and extended surfactants that produces the optimal middle phase microemulsions, and the ‘Cc’ term represents the Cc-values of the surfactants calculated in this work. Shown in Table 9 are the experimental Cc<sub>mix</sub>-values which are in the range of -2.75 to -2.71 and are very similar to the HLD predicted Cc<sub>mix</sub> of -2.76. Moreover, less than 2 % error of the HLD predicted Cc<sub>mix</sub> suggests that the HLD equation can be used for predicting microemulsion systems at the formulation condition with minimal experimental work, once a Cc/K database is compiled.

### Sand Pack Experiment

A sand pack study is performed to evaluate the oil displacement efficiency of the optimized surfactant-only formulation with no added alcohol or polymer at reservoir temperature of 52°C. The optimized binary mixture of C<sub>10</sub>-(PO)<sub>4</sub>-(EO)<sub>1</sub>-SO<sub>4</sub>Na and Steol Cs460 is selected as the chemical flooding solution because it produces low IFT compared to other three optimized surfactant systems that are shown in Figure 5. Figure 6 shows the cumulative oil recovery and the residual oil saturation (Sor) profile. It is worthwhile noticing that the injection of 1 PV, 0.75 wt % total surfactant concentration of surfactant-only slug displaces about 60 % of the trapped oil from the sand packed bed. In addition, the residual oil saturation is reduced from 25 % to about 10 % demonstrating the feasibility of the HLD predicted surfactant-only flood system in a high salinity condition.

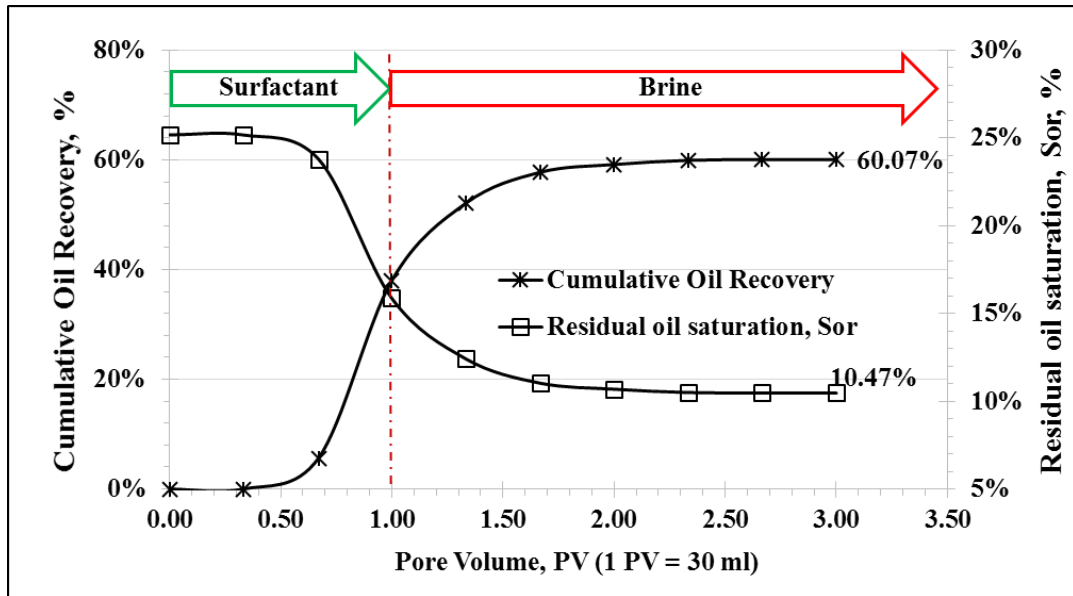


**Figure 6.** Sand packed study: Effect of 1 PV, 0.75 wt. % surfactant slug consisting mixture of C<sub>10</sub>-(PO)<sub>4</sub>-(EO)<sub>1</sub>-SO<sub>4</sub>Na and Steol Cs460 on cumulative oil recovery and Sor reduction.

## Conclusion

In this work, binary mixtures of sodium alkyl alkoxy sulfate and sodium alkyl ethoxy sulfate surfactants are demonstrated to be a promising basis for surfactant formulations for an extremely saline environment. The proposed formulations not only produced a homogeneous clear aqueous phase but also generated ultra-low interfacial tension with the crude oil at the reservoir conditions without use of low molecular weight alcohols or hydrotropes. Sand pack studies further validated the feasibility of the designed formulation by mobilizing 60 % of residual oil even without the incorporation of mobility control agent or the addition of a low molecular weight alcohol to improve coalescence rates.

Moreover, the use of the HLD equation in designing microemulsion systems for cEOR application is demonstrated. A careful determination of HLD parameters such as characteristic curvature, K-value, and temperature constant of the surfactants are found to play an important role in the accuracy of this correlation. To our knowledge, this is the first and only work that has attempted to accurately predict the ratio between two surfactants at which the optimal Type III microemulsions can be formed at the reservoir condition using only the HLD equation. This work demonstrates the screening of surfactants formulation for cEOR can be made much more efficient by significantly reducing the number of experiments and time that are currently being invested in phase behavior studies. The only drawback of such correlations could be its lack of determining aqueous phase stability of the proposed formulation at the formulation condition, which could in theory be addressed by separate studies of precipitation boundaries and coacervation.

## **CHAPTER 3: Single Well Field Feasibility of Surfactant-Only Flooding in Extreme Saline Brine Reservoir**

### **Introduction**

During surfactant based chemical enhanced oil recovery (cEOR) process, the reservoir-injected surfactant slug lowers the interfacial tension (IFT) between the reservoir brine and crude oil and makes conditions favorable to recover entrapped oil from subterranean reservoir rocks<sup>57-58</sup>. Typically, surfactant's performance to mobilize trapped oil depends on the reservoir characteristics such as brine composition, temperature, type of crude oil, and the type of rock matrix<sup>17</sup>. Therefore, it is necessary to tailor surfactant formulation for cEOR application at the site-specific reservoir conditions.

As part of our most recent effort in developing surfactant formulations for matured oil fields in Oklahoma, U.S.<sup>10,41</sup>, one of the key challenges is to explore surfactant candidates for the targeted reservoirs which have extremely high total dissolved solids (TDS) levels in the produced brine (e.g., > 250,000 mg/L). The injected surfactant solution for any cEOR project has to remain chemically stable in subterranean conditions during active pumping operations of chemical flooding, which could last for years<sup>11</sup>. However, the presence of excessive amount of monovalent and divalent cations, Na<sup>+</sup>, K<sup>+</sup>, Mg<sup>2+</sup> and Ca<sup>2+</sup>, in a high TDS brine can make an injected surfactant solution to precipitate or phase separate<sup>14-15, 31</sup>. Both surfactant precipitation and phase separation are undesirable for a cEOR process because not only they increase the IFT but could also plug the formation<sup>38</sup>. In recent years, a series of sodium alkyl ethoxylate propoxylate sulfate surfactants also known as 'extended surfactant' is found to show promising results in high TDS brines<sup>11</sup>. Unlike conventional EOR surfactants, extended surfactants have either propylene oxides (POs) or both POs and ethylene oxides (EOs) functional groups inserted between their

hydrophilic sulfate head groups and hydrophobic carbon tail<sup>34</sup>. The presence of polar groups, EOs and POs in an extended surfactant have three main advantages over conventional surfactants; 1- increase hardness and saline tolerance<sup>11</sup>; 2- enhance surfactant's tail interaction deeper into the oil phase at oil-water membrane, which significantly reduces IFT<sup>34</sup> and; 3- most importantly, the number of POs and EOs functional groups can be tailored to meet the requirements of various reservoir or formulation conditions<sup>12</sup>. Previously, Maerker *et al.*<sup>59</sup> used the combination of two extended surfactants having different number of EOs and POs in order to design a surfactant flood system for the Loudon field site located in Illinois, U.S., that has brine TDS and hardness of about 104,600 ppm (mg/l), and 4,000 ppm respectively. They found the surfactant systems containing extended surfactant to show stable aqueous phase and to generate ultra-low IFT with the crude oil at the reservoir conditions. Another class of surfactants, sodium alkyl ethoxylate sulfates (SAES), are also known to have excellent hardness tolerance<sup>38</sup>. However, these surfactants form viscous microemulsions, gels or liquid crystals, which are undesirable for cEOR application. Therefore, SAES are being used as a co-surfactant in a surfactant mixture to achieve desirable results. Shiau *et al.*<sup>10</sup> developed a surfactant flood system for the SE Hewitt site located in Oklahoma, U.S., which has brine TDS of 102,300 mg/l, using the blend of extended surfactant, SAES, and branched sodium diphenyl oxide disulfonate surfactant. The reported surfactant formulation exhibited stable aqueous phase, generated ultra-low IFT and mobilized 90% of the residual oil during the field trial<sup>60</sup>. Similarly, a ternary blend of sodium sulfosuccinate, SAES, and a branched sodium diphenyl oxide disulfonate has been reported to show promising results in Stewart Fee site located in Oklahoma, US, that has

brine TDS of 165,000 mg/L and a hardness of about 8,500 mg/l<sup>41</sup>. This surfactant system not only showed excellent lab results, stable surfactant aqueous solution and ultra-low IFT with the crude oil at the reservoir condition, but also mobilized 87% of the residual oil during the single well field test. Some authors have also reported the use of co-solvents like isopropanol and sec-butanol to enhance the hardness tolerance of surfactants<sup>39</sup>. However, the risk of increase in IFT as well as the cost limits their use.

This work presents part of designing and field implementation effort for cEOR, specifically, on developing possible alcohol-free and surfactant-only flood formulations that incorporate extended surfactant and SAES for a targeted formation with extreme high level of total TDS of above 300,000 mg/l and total hardness of about 13,000 mg/l in the produced brine. To our knowledge, this is reservoir with the highest TDS brine that has ever been considered for cEOR candidates. A surfactant-only injection protocol for field test is first optimized in the laboratory through sand packed studies. In addition, single well chemical tracer tests (SWCTT) are performed before and after surfactant injection to quantify the oil mobilization efficiency of the surfactant flood system. Moreover, numerical simulation method is applied to accurately analyze data obtained from SWCTT tests.

#### *Background: Single Well Tracer Test (SWCTT)*

SWCTT method is implemented primarily to measure the in- situ residual oil saturation (Sor) of mature oil field that has been water flooded for several years<sup>61</sup>. In recent years this method has also been carried out to determine the Sor before and after enhanced oil recovery (EOR) operations in order to evaluate the effectiveness of EOR agents in a single well pilot<sup>62</sup>. The SWCTT method has gained popularity among oil industries because of



its easy implementation, high success rate, accuracy, and reasonable cost<sup>62</sup>. Additionally, the test is nondestructive meaning after SWCTT test, the reservoir is returned to its initial condition without damaging the formation<sup>63</sup>. There are primarily four standard stages<sup>62</sup> of SWCTT; 1- Partitioning/reactive tracer, usually an ester compound mixed with the reservoir brine is co-injected with the cover tracer and material balance tracer, short chain alcohols; 2- Reactive tracer injected in step 1 is pushed farther away from the wellbore to the desired depth of investigation by injecting pusher brine consisting of only material balance tracer; 3- the well is shut in for specified time during which the hydrolysis of the reactive tracer takes place. The shut-in time depends on the reservoir temperature; 4- Well is back produced and the produced water samples are collected from the well head periodically. The concentration of the tracer in produced water samples are analyzed shortly after their collection, preferably at the on-site portable laboratory using gas chromatography (GC). During the shut-in period, a portion of injected reactive tracer, ester, partitions into the oil phase and the remaining reactive tracer stays in the water phase, which hydrolyzes and forms alcohol and acid. Acids are adsorbed onto the reservoir rocks while the oil insoluble alcohol remains in the water phase. During pullback, the produced alcohol, which doesn't partition into the oil phase, arrives relatively earlier than the oil-partitioned reactive tracer. A lag between the arrival time of reactive tracer and the product alcohol is considered as the basis for  $S_{or}$  determination. The tracer concentration profiles plotted against barrels (bbls) of water produced gives the retardation/lag factor,  $\beta$ , between the product alcohol and reactive tracer. In theory, a wide separation between the peaks of product alcohol and reactive tracer indicates higher  $S_{or}$  in situ and vice versa. In addition, the equilibrium partitioning coefficient of the

selected reactive tracer, K, which provides insight on the solubility preference of reactive tracer for a reservoir oil and brine, is also required for Sor estimation. The K value is determined in the laboratory prior to SWCTT using reservoir brine and crude oil at the reservoir temperature.

Ideally Sor can also be estimated analytically by determining the retardation factor between ester and product alcohol on the plot of tracer concentration versus produced brine. However, the real cases are seldom ideal and to overcome this limitation, numerical simulation methods are implemented<sup>64</sup>. One of the main advantages of numerical simulation method over analytical method is that the simulation is capable to interpret SWCTTs results with complex multi-peaks that could be the result of reservoir heterogeneity or cross flow between layers<sup>65</sup>. Also simulation takes into account the effects of wellbore dead volume and ester reaction during flow<sup>66</sup>. Detailed description regarding SWCTT simulation model and its approach to simulate complex tracer profiles obtained from field tests are reported in literatures<sup>67-68</sup>.

## **Experimental**

### *Materials*

The extended surfactant, C<sub>8</sub>-(PO)<sub>4</sub>-(EO)<sub>1</sub>-SO<sub>4</sub>Na, used in this study for both lab experiments and field tests was provided by Sasol North America Inc., Lake Charles, LA. SAES surfactant i.e., sodium laureth sulfate, trade name Steol Cs460, was purchased from Stepan Chemical Inc. F-95 grade Ottawa sand (60-170 mesh size) used in sand packed studies was purchased from U.S. Silica and the Tracers: ethylformate (>97%), methanol (>97%), and n-propanol (>97%) used in SWCTT tests were purchased from Univar, Oklahoma City, OK.

### *Reservoir Information*

The target W site located near Guymon, Oklahoma is the oil field of interest where SWCTTs were performed. The produced reservoir brine and crude oil samples retrieved from the site were used for the lab experiments. Table 10 shows information on composition of the reservoir brine. Brine compositional analysis was performed by the Red River laboratory of Oklahoma City, OK.

**Table 10.** Formation Brine Analysis

<b>Components</b>	<b>Concentration (mg/l)</b>
Sodium	51675
Potassium	1076
Magnesium	2868
Calcium	10105
Iron	10
Sulfate	341
Chlorine	235634
Total hardness (Ca <sup>2+</sup> and Mg <sup>2+</sup> )	<b>12973</b>
Total dissolved solids	<b>301710</b>

The permeability, porosity, pay thickness, and crude oil viscosity of the War Party site are reported as 500 to 1000 mD, 15-20 %, 12 ft, and 4.5 cP at the reservoir temperature of 52°C (125 °F) respectively. The estimated wellbore dead volume is 35 bbls and the average production rate during the test is 55 bbls/day.

### *Sand Pack Study*

A glass chromatographic column that is 1 inch in diameter and 6 inches long was used for sand pack studies. The F-95 grade Ottawa sand was used as a column packing material. The detailed information on procedures that were followed during packing sand and preparing column for a chemical flood are found elsewhere [Chapter 1]. The pore

volume (PV), which is also known as void volume of sand pack, was calculated by conducting the salinity gradient test. The column was first saturated with 2 wt % NaCl solution followed by saturation with the reservoir brine. Effluent samples were collected for every 3 mL immediately after brine injection was initiated. The conductivity of each effluent sample was measured and the plot of normalized conductivity against volume injected was constructed. A breakthrough of any conservative chemical solution that is injected into a sand pack occurs at one PV. In accordance with this concept and from the conductivity vs. volumes injected plot, the PV of the sand packs used in this study was determined to be  $29 \pm 2$  ml.

#### *Partitioning Coefficient and Hydrolysis Rate Constant*

The partitioning/reactive tracer coefficient, K, measurement was carried out by preparing four sample replicates; each containing equal volumes, 10 mL each of filtered brine and oil. The reactive tracer concentration in brine was 10,000 ppm. All samples were placed in the shaker that was set to 350 rpm and were shaken for at least an hour. Next, the samples were placed inside oven ( $52^{\circ}\text{C}$ ) to equilibrate. After 1 hour, in every  $30 \pm 5$  minutes, aqueous phase samples were collected from the bottom of the vials and the reactive tracer concentration of each sample was determined using gas chromatography (GC). The equilibrium partition coefficient K was calculated from the ratio of reactive tracer concentration in oil to the concentration in water.

The hydrolysis rate constant of reactive tracer to form alcohol is strictly dependent on reservoir temperature and is typically assumed to follow the pseudo-first order reaction<sup>67</sup>. Sample preparation and analysis technique to determine hydrolysis rate constant of

reactive tracer were similar to that of partitioning coefficient determination. The first order reaction is:

$$\ln[A]_t = -kt + \ln[A]_0 \quad \text{Equation (1)}$$

Where  $[A]_t$  is the concentration of tracer at time t,  $[A]_0$  is the initial known concentration of tracer, and k is the rate constant which is the slope of “ $\ln[A]_t$  versus t” plot.

### *SWCTT Field Operation*

SWCTT field operations were designed based on target volume or PV, approximately 85 bbls, of the investigation region that was characterized with radius distance of 9 feet from the well bore, pay zone thickness of 12 feet, and assumed porosity of 20 %. Table 11 summarizes the details of field operational steps.

**Table 11.** Field operational steps and amount of chemicals injected, 1 PV = 85 bbls

		<b>W Site</b>	
<b>Step</b>		<b>Injected fluid</b>	<b>Chemicals</b>
<b>Water Flooding</b>		Brine 6 PV	
<b>SWCTT</b>	Reacting tracer	0.28 PV	EthylFormate 10,000 ppm Methanol 5,000 ppm n-propanol 5, 000 ppm
	Pusher	1.13 PV	Methanol 5,000 ppm
	Shut in	18 hrs	
	Pull-back	1.6 PV	
<b>Surfactant only Flooding</b>		0.5 PV, 0.5 wt %	
<b>Water Flooding</b>		4. 3 PV	
<b>SWCTT</b>	Reacting tracer	0.28 PV	EthylFormate 10,000 ppm Methanol 5,000 ppm n-propanol 5, 000 ppm
	Pusher	1.13 PV	Methanol 5,000 ppm
	Shut in	18 hrs	
	Pull-back	2 PV	

Field operation of SWCTT was divided into four major events. The first event was the baseline water flooding in which 6 PVs of recycled reservoir produced brine was injected at the average rate of 150 bbls/day. This step was carried out to achieve minimum Sor of the target volume around the well bore. The second event was the pre-chemical tracer test and was carried out to confirm the Sor of the target region. The third event was the surfactant only flooding in which laboratory designed surfactant flood system was injected into the reservoir with a brine pusher to move the mobilized oil further away from the wellbore. The fourth and final event involved post-chemical tracer test in which the final Sor of the target zone was determined. Ethylformate was chosen as the reactive/partitioning tracer for SWCTT operations because the reservoir temperature is below 130 °F<sup>62</sup>. Methanol was used as the material balance tracer and the n-propanol was used as the cover tracer.

A cover tracer is usually incorporated with the reactive tracer slug to keep track of water that contains ester. It is also included to overcome any unforeseen circumstances such as complete hydrolysis of the reactive tracer<sup>62</sup>. In such circumstance, Sor cannot be evaluated because the retardation factor,  $\beta$ , cannot be determined. However, the cover tracer, n-propanol, which is found to arrive at the same time as the ethylformate during pullback allows to calculate Sor by determining  $\beta$  between the peaks of n-propanol and ethanol even if all of the ethylformate injected is hydrolyzed. Therefore, sometimes cover tracers are also called as insurance tracer.

#### *SWCTTs Data Interpretation Method*

A similar simulation method reported by Jin *et al.*<sup>60</sup> in their work was adapted in this work to interpret field data. The SWCTTs results were interpreted using the CMG-

STARS software. A 2D radial model with a constant grid block size of 0.01 m was used to model the tests. Also for simplicity purpose, following assumptions were made; constant reservoir temperature, no crossflow between layers, no fluid drift, and no effect of pH variation on ester hydrolysis reaction. Other critical variables such as K-value and reaction rate constant of the reacting tracer required for simulation were measured in the lab at the reservoir conditions.

The injection and production schemes similar to field operation were used as simulation inputs and the injected tracer concentration was tuned to match the recovery history of tracers. The number of layers and individual flow fraction in each layer were used as the key matching parameters to model the irreversible flow. In addition, lab measured hydrolysis reaction rate was used as input and was tuned later for better fitting. The dispersivity coefficient was used to match the shape of the tracer profiles. Finally, the residual oil saturation, which is the objective of the simulation work, was tuned to accurately represent the tracer peak location.

The residual oil saturation,  $S_{or}$ , in each layer is given by<sup>61-62</sup>:

$$S_{or} = \frac{\beta}{\beta+K} \quad \text{Equation (2)}$$

Where  $\beta$  is the retardation factor between product alcohol and reactive tracer, ester, and  $K$  is the equilibrium partition coefficient of the reactive tracer

$$\beta = \frac{Q_A}{Q_B} - 1 \quad \text{Equation (3)}$$

Where  $Q_A$  and  $Q_B$  are the produced volumes at which the ester and alcohol peaks appear respectively.

## Results and discussions

### *Surfactant Formulations*

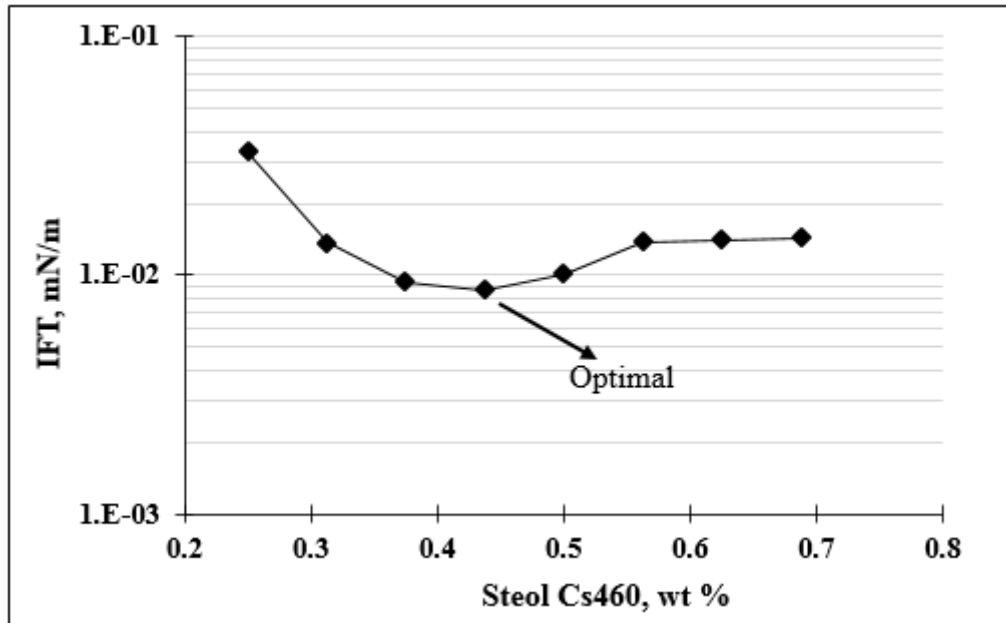


**Figure 7.** Equilibrium IFT measurements of the binary mixtures ( $C_8-(PO)_4-(EO)_1-SO_4Na$ , 0.25 wt % + SAES) with the reservoir crude oil at 52°C

Four optimized surfactant formulations have been developed and proposed for this specific W site reservoir conditions by the hydrophilic lipophilic deviation (HLD) method and is discussed elsewhere [Chapter 1]. During the field tasks planning stage, the surfactant formulation incorporating  $C_8-(PO)_4-(EO)_1-SO_4Na$  and SAES was chosen as the surfactant flood system for further field test because of unavailability of other three extended surfactant candidates in bulk quantity. Figure 7 shows the IFT measurements of the surfactant system at the various concentrations of SAES. The ratio between  $C_8-(PO)_4-(EO)_1-SO_4Na$  and SAES at which the minimal IFT, 8E-3 mN/m, is obtained is defined as the optimal formulation. The aqueous surfactant solution at the optimal condition exhibits clear homogeneous single-phase solution for extended period. Also the coalescence rate of  $C_8-(PO)_4-(EO)_1-SO_4Na/SAES/crude$  microemulsions at the optimal



condition is reported to be less than 30 minutes showing that the proposed  $C_8-(PO)_4-(EO)_1-SO_4Na/SAES$  blend satisfies the criteria<sup>12, 54</sup> of the cEOR surfactant flood system.

### *Sand Pack Experiments*

Sand pack studies are conducted in laboratory for the purpose of optimizing surfactant-only flood system under flow through conditions prepared for the field test. The optimal Type III microemulsion formulation described in previous section which exhibits minimum IFT value in Figure 7 is chosen for the sand pack tests. The resulted IFTs of the surfactant slugs with the crude oil were confirmed before injecting into the sand pack. The IFT values for each column test are presented in Table 12. It can be observed that all the surfactant slugs produce ultra-low IFT.

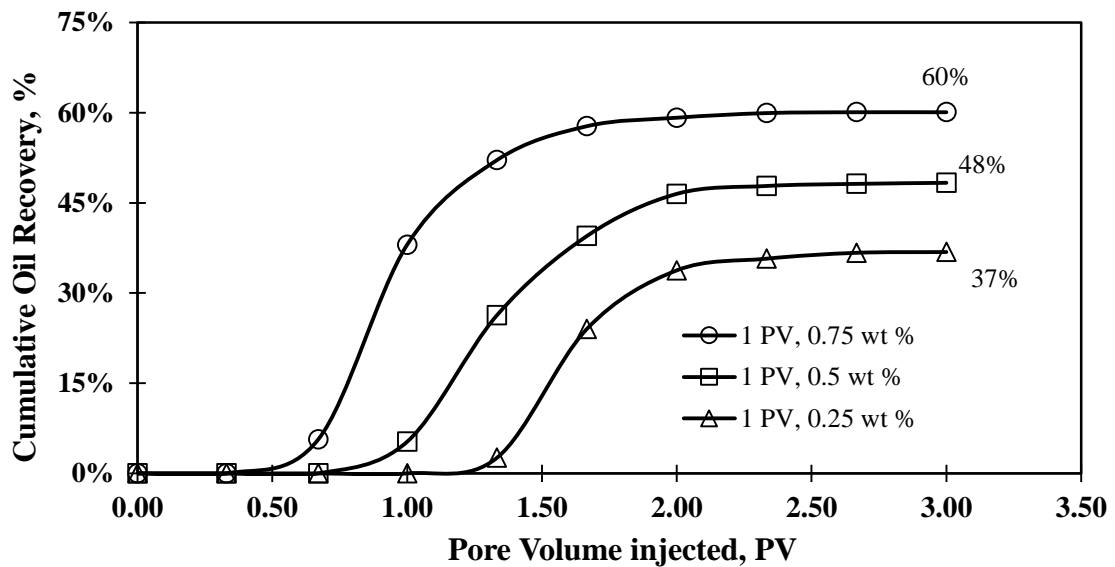


**Figure 8.** Effect of surfactant concentration on cumulative oil recovery and oil break through. Post water flooding surfactant injection (1 PV)

Figure 8 shows the effect of varying total surfactant concentration on cumulative oil recovery. As seen in the Figure, decreasing the overall surfactant concentration from 0.75 wt % to 0.50 wt % decreases the cumulative oil recovery from 60% to 48%. A further decrease, down to 37%, in oil recovery is observed for 0.25 wt % surfactant concentration.

Figure 8 also shows early oil breakthrough for the sand pack that is flooded with the surfactant concentration of 0.75 wt % compared to that of sand packs flooded with less concentrated surfactant slug.

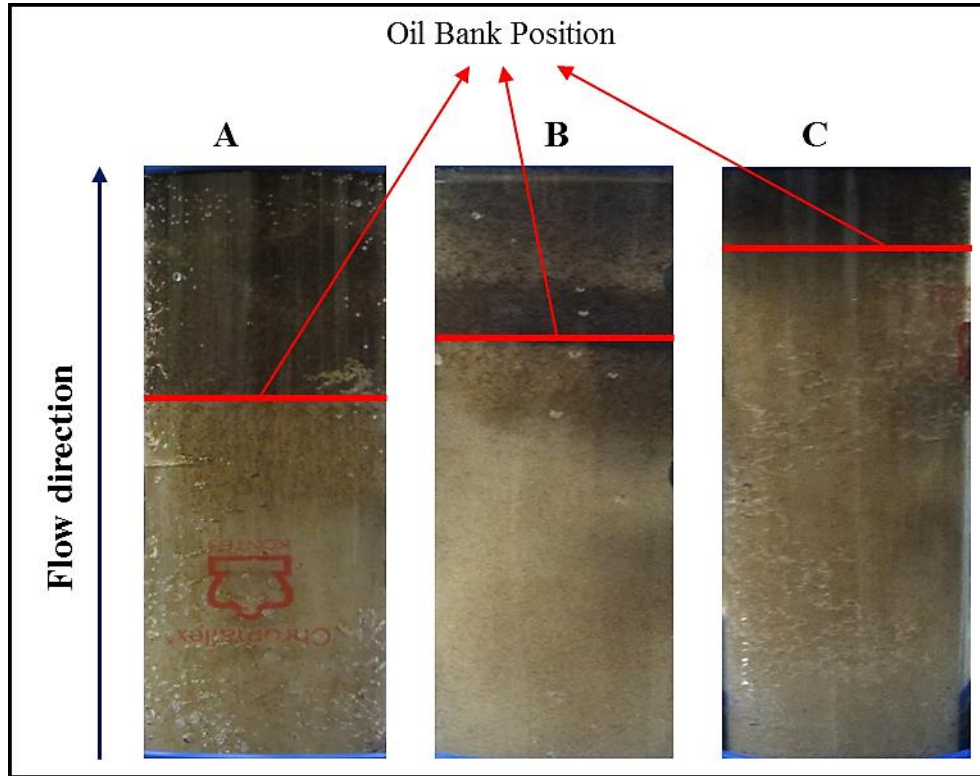


**Figure 9.** Effect of surfactant concentration on oil bank position. **A)** 1 PV, 0.25 wt% **B)** 1 PV, 0.50 wt% **C)** 1 PV, 0.75 wt%. Fluid injection rate: 0.3 ml/min.

Figure 9 shows the position of oil bank in sand pack shortly after flooding with one PV of each surfactant slug. It is observed that the sand pack flooded with 0.75 wt % surfactant slug has relatively higher oil bank advancing position than that of 0.50 wt % and 0.25 wt % surfactant slugs respectively. In ideal case where the surfactant adsorption in porous media is negligible and if significant IFT reduction at the oil-water interface is the only oil recovery mechanism, then lowering overall surfactant concentration while maintaining the optimal Type III region should not decrease the cumulative oil recovery and nor should it delay the oil breakthrough. However, the observation made in this study

doesn't correspond to the ideal case. One potential explanation could be the severe surfactant retention in porous media by adsorption. In literature it is reported that the oil recovery is sensitive to the amount of surfactant injected and that the amount of surfactant required depends on the level of adsorption in porous media<sup>69</sup>. In such case, a 0.75 wt % surfactant slug is arguably the best among other two less concentrated surfactant slugs as most surfactants are available to effectively participate in oil recovery mechanism. It is also likely that 0.75 wt % slug traverses in porous media faster because of more surfactant availability even after adsorption to mobilize oil resulting in faster oil bank formation and ultimately leading to the early oil breakthrough.

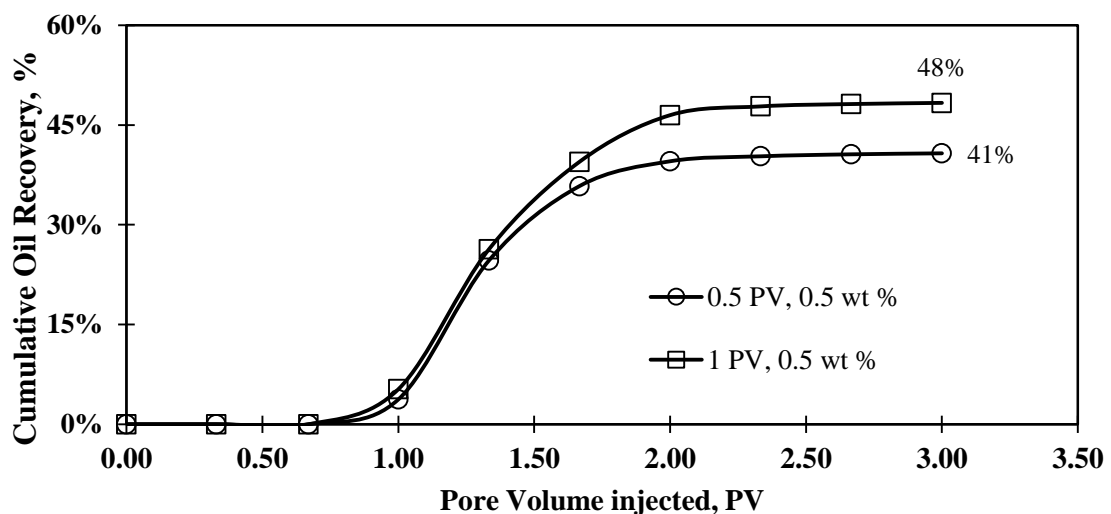


**Figure 10.** Effect of surfactant slug size on cumulative oil recovery. Post water flooding surfactant injection (1 PV)

Figure 10 shows the effect of varying the size of surfactant slug (in PVs) on cumulative oil recovery. The total surfactant concentration of each slug is constant at 0.5 wt %. As seen in the Figure 10, 1 PV of surfactant slug recover 48% of residual oil, which is slightly higher compared to 41% of residual oil recovered by a 0.5 PV surfactant slug. A possible explanation for the lower oil recovery with 0.5 PV surfactant slug is surfactant dilution. It is likely that the oil mobilization efficiency of 0.5 PV surfactant slug could decrease

after being diluted with the chaser brine. This scenario could also be compared and explained with the similar potential reasoning given earlier (See Figure 8) for the less concentrated surfactant slug with less oil recovery. As observed in Figure 10, even though total oil recovery is lower for 0.5 PV surfactant slug, the oil breakthrough time for both 0.5 and 1 PV surfactant slugs are similar. A potential explanation for such observation is the similar effect of both slugs during the early stage of surfactant flood. It is possible that when these two surfactant slugs first come in contact with oil, the effect is similar as both slugs are identical in terms of surfactant concentration. Thus, the effect of smaller slug size, 0.5 PV, is not realized until the dilution begins due to the arrival of the chaser brine and by the time this happens, portion of oil already makes it way to the effluent resulting in similar oil breakthrough front detected at the column outlet regardless of slug size.

**Table 12.** Summary of sand pack studies

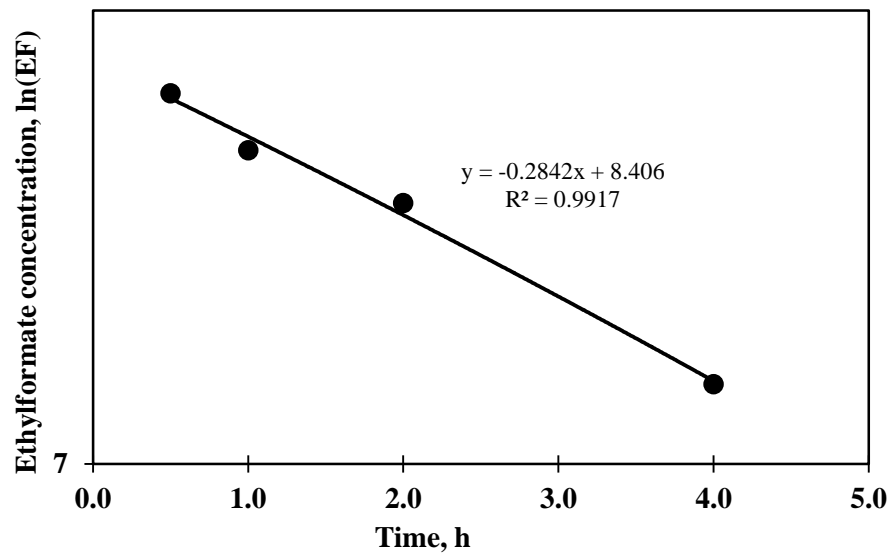
<b>Sand Pack</b>	<b>Surfactant Injection protocol</b>	<b>IFT, mN/m</b>	<b>Initial Sor ± 0.02</b>	<b>Final Sor ± 0.02</b>	<b>Cumulative oil recovery, %</b>
1	1 PV, 0.75 wt %	8.00E-03	0.24	0.10	60
2	1 PV, 0.50 wt %	7.80E-03	0.20	0.10	48
3	1 PV, 0.25 wt %	7.50E-03	0.26	0.16	37
4	0.50 PV, 0.50 wt %	8.1 E-03	0.23	0.14	41

Table 12 summarizes the detailed information of each sand pack test. Taking into account of sand pack performance, field operation, and cost, the surfactant only flood system with slug size of 0.5 PV and 0.5 wt % surfactant concentration is thus decided as cEOR agent for field test. Literature shows that results of sand pack test corresponds very well with

the performance of coreflood test<sup>41</sup>. For this reason, coreflood tests are not performed in this study.

### *Equilibrium Partitioning Tracer Coefficient, K*

It is desired for reactive tracer to have slightly higher solubility preference for oil over brine to estimate the  $S_{or}$  accurately<sup>62</sup>. The equilibrium partition coefficient  $K$  of ethylformate measured in this study is  $2.91 \pm 0.30$ . This value suggests that the ethylformate prefers oil almost 3 times to brine at the reservoir conditions. The ethylformate  $K$  values, which are sensitive to the reservoir temperature, brine salinity, pH, and crude oil light component, are reported to be in the range of 2.0 to 8.0<sup>62, 67</sup>.



**Figure 11.** Ethylformate hydrolysis rate constant study conducted at 52°C

Figure 11 shows the plot of ethylformate concentration versus time under the reservoir temperature. According to the Equation 1, the slope of such plot,  $-0.284 \pm 0.03 \text{ hr}^{-1}$  ( $-7.88\text{E-}5 \pm 8\text{E-}6 \text{ s}^{-1}$ ), is the hydrolysis rate constant of the ethylformate. This value is similar to the rate constant,  $7\text{E-}5 \text{ s}^{-1}$ , reported in literature<sup>60</sup> for ethylformate hydrolysis at the reservoir temperature of 123 °F.

### Field Test Results Interpretation

The matched SWCTT results are shown in Figures 12 and 13 for pre- and post-surfactant injection respectively. The profiles of reactive tracer ethylformate and product alcohol ethanol are well fitted by a single layer model indicating homogeneous geological formation near the test well. Table 13 summarizes the fitting parameters. As observed in the table, the reaction rate of ethylformate decreases from  $9.5E-5 \text{ s}^{-1}$  in pre surfactant SWCTT to  $6.6E-5 \text{ s}^{-1}$  in post surfactant SWCTT. The decrease in rate constant is most likely the result of temperature drop from injecting high volume of cold fluid during the tests<sup>70</sup>. Similar phenomenon is also reported in literature<sup>60</sup>.

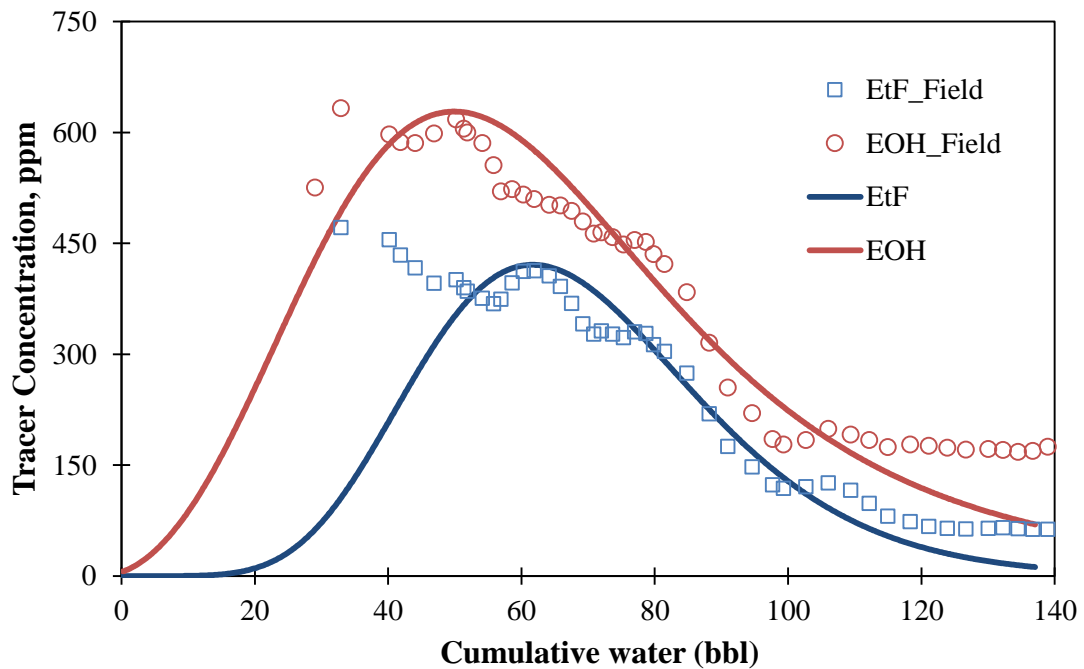


**Figure 12.** Pre Surfactant SWCTT tracer concentration profile; single layer fitting. Software: CMG-STARS

The tracer concentration profile of pre-surfactant SWCTT depicted in Figure 12 shows a narrow separation between the peaks of ethylformate and ethanol. This observation indicates that the  $S_{or}$  after water flooding is low<sup>62</sup> and is further confirmed from

simulation results that shows water flooding Sor of 0.11. It is reported that based on reservoir formation, oil and brine properties, and other unknown variables, the Sor of mature reservoirs could vary from less than 0.1 to more than 0.45<sup>62</sup>. Given the fact that the formation at W site is highly permeable, 500 mD to 1000 mD, it is possible for this specific reservoir to have Sor of 0.11, especially after being water flooded with 6 PVs of reservoir brine at three times higher injection rate than its equilibrium production rate of 55 bbls/day. Increasing the velocity of injection fluid increases the capillary number and thereby decreases the Sor<sup>58</sup>. Furthermore, as observed in Figure 13, there is no distinct separation between the peaks of ethylformate and ethanol in post-surfactant SWCTT indicating that the Sor is very low. The simulation results verify this observation and show the post surfactant Sor of 0.03.

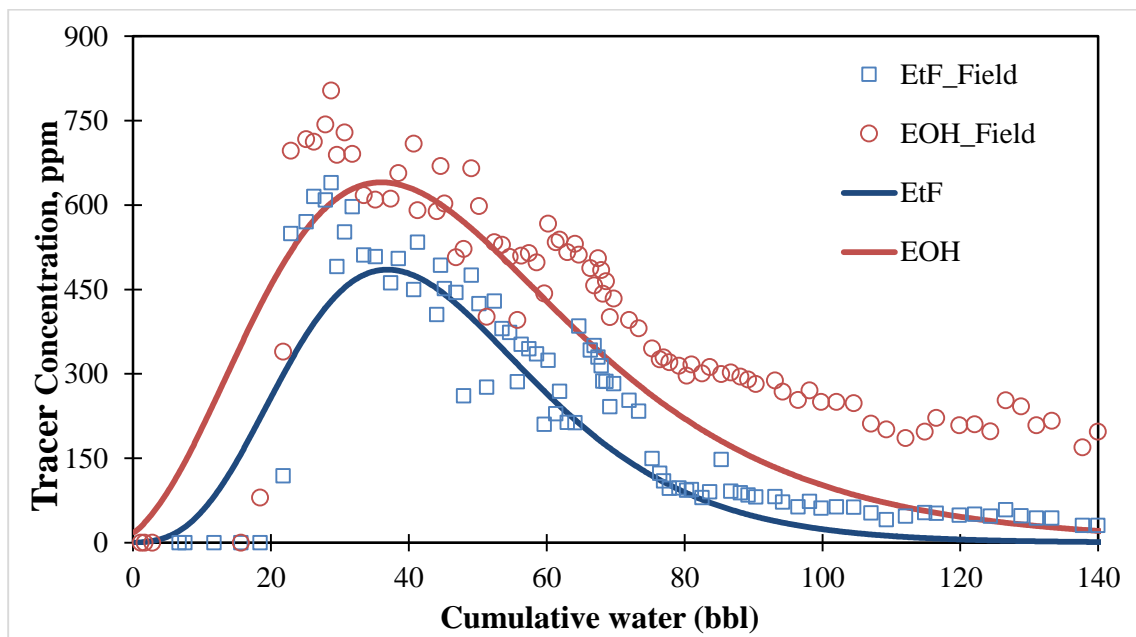


**Figure 13.** Post Surfactant SWCTT tracer concentration profile; single layer fitting. Software: CMG-STARS

**Table 13.** Simulation Matching Parameters. Software: CMG-STARS

<b>Matching Parameter</b>	<b>Pre Surfactant SWCTT</b>	<b>Post Surfactant SWCTT</b>
Thickness (m)	3.66	3.66
Porosity	0.25	0.27
Partition Coef. K	2.91	2.91
Reaction Rate (s-1)	9.50E-05	6.60E-05
Sor = 1 - Sw	0.11	0.03
Dispersion Coef. Ethyl Formate	0.009	0.013
Dispersion Coef. Ethanol	0.009	0.03
Tracer Injection Rate (m3/day)	12.5	13.0
Pusher Injection Rate (m3/day)	27.5	19.0
Production Rate (m3/day)	24.65	22.0

An overall Sor reduction of about 73 % is observed after cEOR in field test, which is slightly higher, compared to the sand pack studies conducted with similar surfactant only injection protocol. However, sand pack studies are only used as a fast pre-screening tool for laboratory designed formulation and its resemblance to the actual reservoir is almost impossible. Jin *et al.*<sup>60</sup> have also reported higher Sor reduction in field test compared to sand pack tests using the surfactant only cEOR system.

### **Conclusion**

Surfactant formulation developed for the ultra-high saline reservoir is optimized in laboratory through sand pack tests and is implemented in field test. Efficiency of the designed formulation in field is verified through SWCTTs and the numerical simulation is applied to interpret field data. Based on the results obtained, following conclusions can be made:



- Surfactant formulation incorporating a blend of extended surfactant,  $C_8-(EO)_1-(PO)_4-SO_4Na$ , and SAES,  $C_{12}-(EO)_3-SO_4Na$  shows excellent aqueous phase stability and generates ultra-low IFT of  $8e-3$  mN/m with crude oil at the reservoir conditions.
- Sand pack studies show improved cumulative oil recovery and early oil breakthrough with increasing surfactant concentration. More surfactants available after reaching surfactant adsorption level to participate in oil recovery mechanism in the case of concentrated surfactant slug could be the potential explanation. Further study is recommended to understand surfactant only flooding systems in sand packs.
- The oil-water partitioning coefficient and hydrolysis rate constant of ethylformate are determined in laboratory and are found to be  $2.91 \pm 0.30$  and  $7.88E-5 \pm 8E-6$  s<sup>-1</sup> respectively.
- The reaction rate constant of ethylformate is found to decrease from  $9.5e-5$  s<sup>-1</sup> in pre surfactant SWCTT to  $6.6e-5$  s<sup>-1</sup> in post surfactant SWCTT. Temperature drop due to high volume cold fluid injection along with pH drop due to product acid of ester reaction could have resulted in such decrease in rate constant.
- High permeable reservoir formation and high injection rate of water flooding could have resulted low Sor of 0.11 in pre surfactant SWCTT.
- The Sor of 0.03 in post surfactant SWCTT and 73% overall Sor reduction demonstrate that the laboratory optimized surfactant formulation is very promising and effective in mobilizing residual oil in ultra -high TDS reservoir.

# CHAPTER 4: Improved Oil Recovery by Reducing Surfactant Adsorption with Polyelectrolyte in High Saline Brine

## Introduction

In surfactant aided chemical enhanced oil recovery (cEOR) techniques, an injected surfactant solution mobilizes trapped oil by lowering the interfacial tension (IFT) of the oil-water interface<sup>28, 56-57</sup>. This technique is proven to recover trapped oil that cannot be extracted using the traditional water flooding method<sup>41</sup>. Despite the potential of surfactant based hydrocarbon extraction, there are still challenges that need to be addressed to make this process economically feasible. Included in those challenges is the issue of surfactant loss due to adsorption on reservoir rock<sup>71-72</sup>. Surfactants that are adsorbed on an oppositely charged rock surface do not lower the IFT of the oil-water interface, and therefore are not available to participate in oil mobilization. This

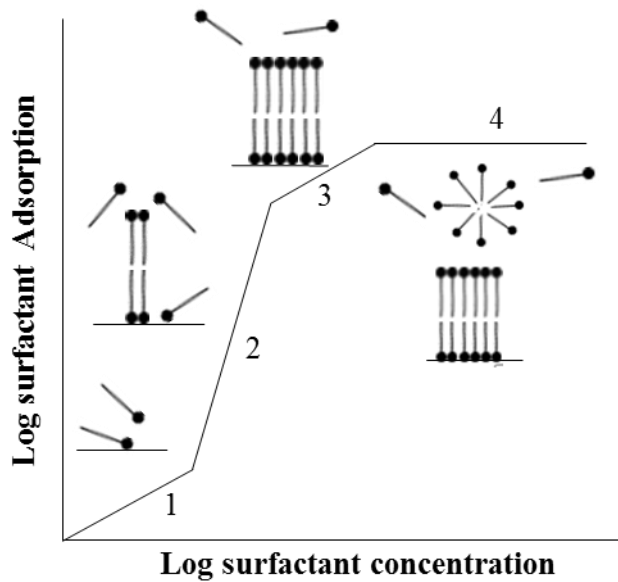


**Figure 14.** Surfactant Adsorption Isotherm

phenomenon lowers the overall efficiency of surfactant based cEOR techniques and increases the cost of projects. Therefore, it is necessary to mitigate surfactant loss on mineral rocks to make cEOR processes economically viable.

The physical adsorption of ionic surfactant on oppositely charged mineral oxide exhibits a low surface coverage region (Region “1” in Figure 14) at low surfactant concentration<sup>73-74</sup> which is described by Henry’s law<sup>75</sup>. At any surfactant concentration above the critical admicelle concentration (CAC), the low coverage region enters to the sharp positive slope region (Region “2” in Figure 14) where the formation of surfactant aggregates such as hemimicelle (monolayer), admicelle (bilayer), or mixture of both may take place<sup>74, 76</sup>. The formation of a bilayer/admicelle, which is the result of surfactant hydrophobic tail-tail interaction, then starts to slow down surfactant adsorption due to saturation of high energy patches on the surface, and enters to the region (Region “3” in Figure 14) where bilayer patches are slowly filled until a complete bilayer is formed<sup>77</sup> or the CMC is reached. This then leads to the plateau region<sup>78</sup> (Region “4” in Figure 14) where surfactant adsorption is constant for any concentration of surfactant above the critical micelle concentration (CMC). Although the formation of the surfactant bilayer prevents additional surfactant adsorption, this is not desirable for a cEOR process because the amount of surfactant that is required to form such a bilayer might be above the economical limit. Therefore, surfactants having the same charge as the reservoir rocks are generally used to minimize surfactant bilayer/admicelle formation. For example, anionic surfactants are typically used for the negatively charged surfaces of sandstone reservoirs and cationic surfactants are typically used for positively charged carbonate reservoirs. However, due to complexities of the reservoirs including rock composition, the presence of clays, brine salinity, multivalent ions, and pH, there is still a possibility of surfactant loss due to adsorption.

Efforts have been made to minimize the surfactant adsorption on rock or soil surfaces. Alkalis such as sodium hydroxide or sodium carbonate are typically used as a chemical agent to lower the adsorption of anionic surfactants<sup>7, 18</sup>. Addition of alkali increases the pH, resulting in an increased net negative surface charge, and thereby reduces the adsorption of anionic surfactants due to electrostatic repulsion. In spite of a positive influence of alkali in lowering adsorption of anionic surfactants, it is limited to reservoirs with low TDS brines; this is mainly because alkalis are sensitive to divalent cations,  $\text{Ca}^{2+}$  and  $\text{Mg}^{2+}$ , and the elevated level of such ions present in high TDS brine causes alkali to precipitate and thus make it ineffective<sup>79</sup>.

Several authors have reported the application of polyelectrolytes as sacrificial agents in reducing adsorption of ionic surfactants on oppositely charged surfaces<sup>21, 27</sup>. It is believed that polyelectrolytes, when adsorbed on the surface, cover positive sites and eliminates electrostatic-attraction driven surfactant adsorption. ShamsiJazeyi *et al.*<sup>21</sup> studied the effect of sodium polyacrylate on adsorption of anionic surfactant. They observed that higher molecular weight (>4500 Da) sodium polyacrylates significantly reduce the adsorption of anionic surfactant on both Brea sandstone and Carlpool dolomite rock surfaces. ShamsiJazeyi also claimed that the presence of surfactant does not affect the adsorption of polyacrylate due to its low desorption and high surface coverage nature. Additionally, they observed that increasing salinity as well as  $\text{Ca}^{2+}$  ions elevates surfactant adsorption on Brea sandstone even in the presence of polyelectrolyte. Other experiments performed by Weston *et al.*<sup>27</sup> showed that addition of another anionic polyelectrolyte, polystyrene sulfonate (PSS), on positively charged metal oxide, alumina, and cationic polyelectrolyte, polydiallyl dimethyl ammonium, on negatively charged

metal oxide, silica, reduced the adsorption of anionic and cationic surfactants, respectively. Weston also observed that a sequential addition methodology -- addition of polyelectrolyte followed by surfactant -- is more effective in reducing surfactant adsorption than simultaneous addition, where polyelectrolyte and surfactant are added together. The hypothesis proposed for this observation is that during sequential addition, the polyelectrolyte does not have to compete with surfactant to adsorb on the metal oxide surface.

It is well known that an increase in electrolyte concentration of a solution increases the adsorption of anionic surfactants<sup>80</sup>. Even though polyelectrolytes are proposed to significantly minimize surfactant adsorption on rocks or metal oxides, their effectiveness in high electrolyte/TDS (> 200,000 mg/l) reservoir brine condition is yet to be studied. A possible explanation may be the difficulties in developing surfactant formulations that remains stable in a very high TDS solution. This work hopes to fill such a gap and demonstrate that polystyrene sulfonates (PSSs) can be used as sacrificial agent in minimizing adsorption of anionic surfactant in a sandstone reservoir that has brine with total TDS of 301,710 mg/l and total hardness ( $\text{Ca}^{2+}$  and  $\text{Mg}^{2+}$ ) of 12,973 mg/l.

## **Experimental**

### *Materials*

Polystyrene sulfonates (PSS) with four different molecular weights (MWs) i.e., 20 KDa (25% active), 70 KDa (30% active), 250 KDa (30% active), and 1 MDa (25% active) are the anionic polyelectrolytes used in this study. These polyelectrolytes are commercially available and were provided by Akzo Noble Inc. Nashville, TN. The 20 KDa (SSMA) polyelectrolyte is reported as the mixture of styrene sulfonates and maleic acid (MA) by the manufacturer. The surfactant system used in this study is the mixture of sodium alkyl

ethoxylate propoxylate sulfate (extended surfactant) and sodium alkyl ethoxy sulfates (SAES) surfactant system reported elsewhere [Chapter 1]. The extended surfactant (32.2 % active), C<sub>10</sub>-(EO)<sub>1</sub>-(PO)<sub>4</sub>-SO<sub>4</sub>Na, was provided by Sasol North America Inc, Lake Charles, LA and the SAES surfactant, trade name Steol Cs460 (60% active), was purchased from Stephan Chemical Inc. All chemicals were used as received without further purification.

**Table 14.** Composition of Brea Sandstone and Ottawa Sand. Information provided by supplier

Components	Brea Sandstone	Ottawa Sand
SiO <sub>2</sub>	93.13 %	99.77 %
Al <sub>2</sub> O <sub>3</sub>	3.86 %	0.051 %
Fe <sub>2</sub> O <sub>3</sub>	0.11 %	0.026 %
FeO	0.54 %	-
MgO	0.25 %	-
CaO	0.10 %	-

Adsorbents that were used in this study are F-95 grade Ottawa sand and Brea sandstone. The F-95 grade Ottawa sand (50-200 mesh) was purchased from Axner Pottery Supply, Oviedo, FL and the Brea sandstone rocks were purchased from Cleveland Quarries, Vermilion, OH. Detail information about the composition of each adsorbent are presented in Table 14. The Brea sandstone rock was further crushed and 35-100 mesh size was selected for study after sieving. The reservoir fluids, brine and crude oil, were collected from a well site located near Guymon, Oklahoma. Complete analysis of both fluids are reported in our other work [Chapter 2].

### *Equilibrium Adsorption Study*

Equilibrium adsorption studies were carried out by introducing 15 g of aqueous phase, brine or 1 wt % NaCl, containing surfactant and/ or PSS into the 5 g of adsorbent, Brea or Ottawa sand, filled vials. The initial surfactant concentration of the aqueous phase was set at 0.75 wt % while the PSS concentrations were varied from 0.1 to 0.8 wt % of sand used. All the samples were left to equilibrate for 24-30 h during which they were constantly shaken in a shaker at 300 rpm. After equilibration, each sample was centrifuged and the aqueous phase was analyzed using high performance liquid chromatography (HPLC). The surfactant and PSS concentration of aqueous phase were determined using conductivity and UV detectors respectively. Similar to Weston <sup>27</sup>, two different sample preparation methodologies, sequential addition and simultaneous addition, were employed for samples that contained both PSS and surfactant. In the sequential addition method, PSS solution were added to the sand and allowed to equilibrate for over 24 h before adding surfactant, whereas the simultaneous addition method involved addition of both PSS and surfactant solution onto the sand at the same time. All experiments were performed at the room temperature and at pH 6.4 and 6.9 for systems with reservoir brine and 1 wt % NaCl water, respectively.

### *Dynamic Adsorption Study*

Glass chromatography columns packed with sand (Brea sand or Ottawa sand) are used for dynamic adsorption studies. The dimensions of each sand pack bed are 3 inches long and 1 inches diameter. Salinity gradient tests similar to that described in our previous work were carried out to determine pore volumes (PVs) of sand packs [Chapter 3]. Each sand pack was flushed with at least two pore volume of reservoir brine before injecting

surfactant and/ or PSS. In addition, sequential addition and simultaneous addition methods were also employed in this study for cases that involved injection of both PSS and surfactant in to sand packs. The fluid injection rate was kept constant at 3 ml/min unless otherwise noted and the experiments were carried out at room temperature.

### *Sand Pack Experiments*

Sand pack studies were conducted at the reservoir conditions to evaluate the impact of lowering surfactant adsorption due to PSS on oil mobilization from porous media. These studies were performed using sand (Brea sand or Ottawa sand) packed glass chromatography columns that are 6 inches long and have 1 inch diameter. Detailed explanation about the steps that were followed during sand packing and preparing oil saturated sand packs for water flooding and surfactant injection are reported elsewhere [Chapter 1]. Oil saturated sand packs were first flooded with reservoir brine (pH = 6.4) until the effluent oil volume was less than one percent of each of the collected sample's total volume. After brine/water flooding, one PV of PSS solution was introduced into each sand pack. The concentration of PSS was varied and was based on the amount of sand. After PSS injection, sand packs were flushed with one pore volume of brine before surfactant injection. Each fluid was injected at the rate of 0.3 ml/min.

## **Results and discussions**

### *Equilibrium Adsorption of Surfactant without Polyelectrolyte*

Figure 15 shows the result of equilibrium adsorption studies of surfactant without polyelectrolyte on both Brea sandstone and Ottawa sand. It can be observed that the surfactant adsorption on Brea sandstone is almost 5 times higher than that on Ottawa sand in reservoir brine (pH = 6.4). This behavior is attributed to the compositional contents of two different sands, which are illustrated in Table 14. As shown in Table 14, Brea



sandstone contains about 93% of silica and 4% of alumina. In contrast, Ottawa sand is composed of 99.8% silica and trace amount of alumina. The net surface charge of mineral oxides strongly depends on solution pH; that is, at certain pH below the point of zero charge ( $\text{pH}_{\text{pzc}}$ ) of the mineral oxide, the net surface charge is positive and at pH above  $\text{pH}_{\text{pzc}}$ , the net surface charge is negative<sup>81</sup>. A typical  $\text{pH}_{\text{pzc}}$  of silica and alumina is around 3.7<sup>82</sup> and 9.1<sup>83</sup> respectively. Therefore, Brea sandstone, which contains about 4% of alumina, shows increased surfactant adsorption due to electrostatic attraction driven surfactant adsorption on positively charge alumina surface compared to negligible alumina-containing Ottawa sand.

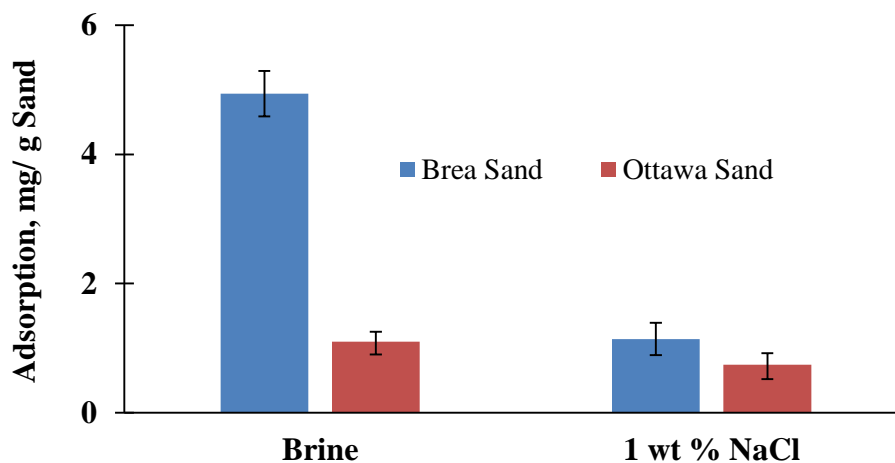


**Figure 15.** Equilibrium surfactant adsorption without polyelectrolyte in two different salinity environment

Figure 15 also shows that the surfactant adsorption on Brea Sandstone in reservoir brine is about three times more than that in 1% NaCl solution ( $\text{pH} = 7$ ). In addition, extremely high surfactant adsorption of about 5 mg/g on Brea sandstone is observed in the reservoir brine. These observations can be explained due to the fact that the TDS of reservoir brine is extremely high. Increase in brine TDS/ electrolyte generally increases the adsorption of anionic surfactant<sup>50, 80</sup>. This is mainly due to the adsorption of cations, especially  $\text{Ca}^{2+}$

and  $Mg^{2+}$  present in high TDS brine, onto the negatively charged sand surface, which results in more positively charged sites for anionic surfactant to adsorb. Similar behavior is also observed in the case of Ottawa sand even though the difference is not as prominent compared to Brea sandstone.

*Equilibrium Adsorption of Polyelectrolytes without Surfactant*

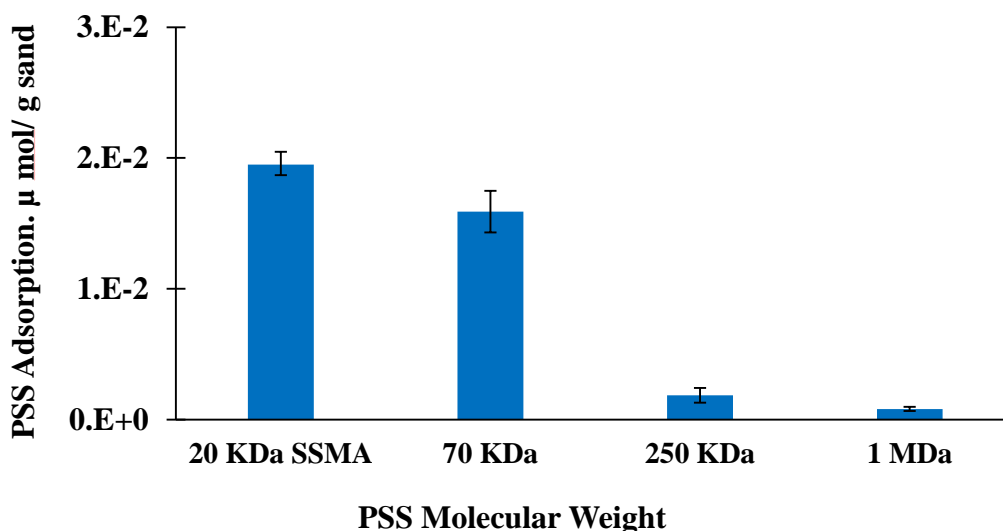


**Figure 16.** Equilibrium PSS adsorption without surfactant on Brea Sandstone at reservoir brine

Ability of a polyelectrolyte to reduce surfactant adsorption depends on its tendency to adsorb onto sand or metal oxides<sup>21, 84</sup>. To understand such phenomenon, the equilibrium adsorptions of four different MW PSSs are studied in reservoir brine (pH = 6.4) using Brea sandstone as an adsorbent. These results are presented in Figure 16. It has been reported that low MW polyelectrolytes adsorbs more on oppositely charged porous adsorbent than high MW polyelectrolyte<sup>84</sup>. The reasoning is that smaller molecules can easily get access to the majority of adsorption sites that are located in pores, which might not be accessible to larger molecules. Similar reasoning can also be used to explain the observations made in our experiments where the adsorption of 20 KDa SSMA on porous Brea sandstone is about 1.95E-2 μmol/g sand and the adsorption decreases with the

increasing PSS MW. In addition, higher MW PSS being densely charged may require larger oppositely charged surface area to adsorb than less densely charged low MW PSS. Since Brea sandstone is mostly composed of negatively charged silica (93%) and very few positively charged alumina sites (4%), it has very limited adsorption sites for PSS to adsorb compared to pure alumina. Therefore, low MW PSSs that require less charged surface area on sand to adsorb may have been favored for adsorption over larger surface area requiring high MW PSSs.

*Equilibrium Adsorption of Surfactant with Polyelectrolyte.*

The effectiveness of PSSs in lowering surfactant adsorption is evaluated by conducting separate equilibrium surfactant adsorption study in the presence of each PSS. These experiments are carried out in reservoir brine using Brea sandstone as an adsorbent. In addition, both sequential and simultaneous surfactant/PSS addition techniques are employed.

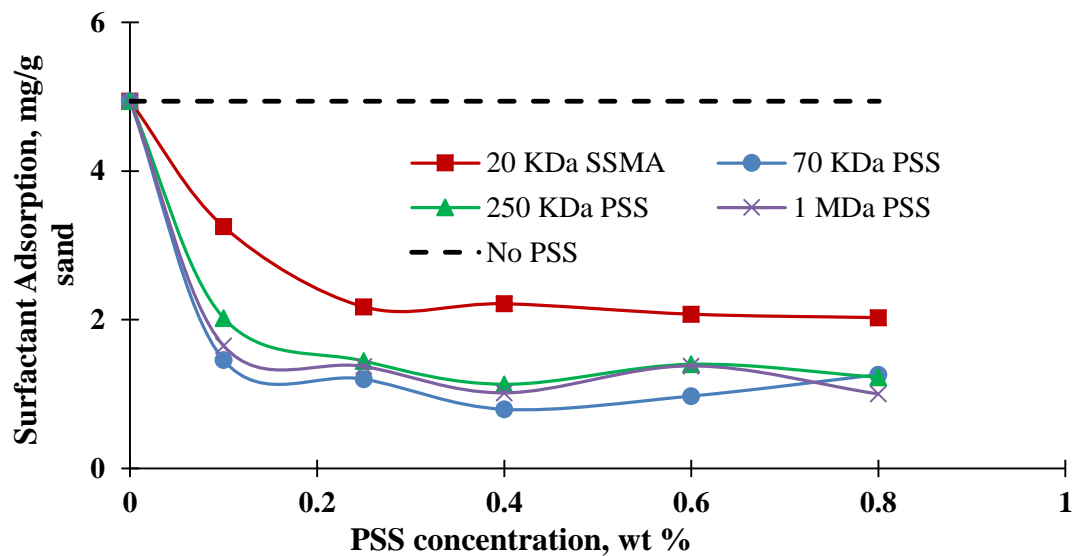


**Figure 17.** Effect of polyelectrolyte on equilibrium adsorption of surfactant on Brea Sandstone at reservoir brine.

Figure 17 shows the equilibrium surfactant adsorption data obtained by employing sequential surfactant/PSS addition technique. It is observed that adding 0.1% PSSs, regardless of their MW, reduces the surfactant adsorption from 5 mg/g sand to less than 2 mg/g sand. In spite of this, most noticeable observation can be made in the case of 20 KDa SSMA. According to the Figure 16, 20 KDa SSMA show higher adsorption on adsorbent compared to other PSSs. Normally, higher adsorption of negatively charged polyelectrolyte on oppositely charged adsorbent results in less adsorption of anionic surfactant due to increased electrostatic repulsion<sup>84</sup>. However, results shown in Figure 17 do not correspond to such a theory as 20 KDa SSMA is found to be the least effective PSS compound in minimizing surfactant adsorption. Two possible explanations are proposed to explain this observation. First, the surface charge density of 20 KDa SSMA is much lower compared to high MW PSSs. This may have decreased the overall effectiveness<sup>21</sup> of 20 KDa SSMA. Second, 20 KDa SSMA is a copolymer that consists of styrene sulfonate (SS) and Maleic acid (MA) segments. MA is a strong acid (pKa = 1.91 and 6.33<sup>85</sup>) and if added to the solution might decrease the solution pH. To verify this, 2000 ppm of 20 KDa SSMA was added in Brine. The result showed that the brine pH dropped from 6.4 to 5.6. Adsorption of anionic surfactant on oppositely charged mineral oxide, alumina (pH<sub>pzc</sub> = 9.1), increases with the decrease in pH<sup>79-80</sup>. Therefore, the presence of solution pH lowering MA block of a copolymer may have lowered the overall effectiveness of 20 KDa SSMA by enhancing surfactant adsorption. Figure 17 also shows that in spite of low adsorption of 250 KDa PSS and 1 MDa PSS on Brea sandstone, as shown in Figure 16, these two polymers are as effective as 70 KDaPSS in

decreasing surfactant adsorption. This behavior is attributed to the high surface charge density of high MW polyelectrolytes.

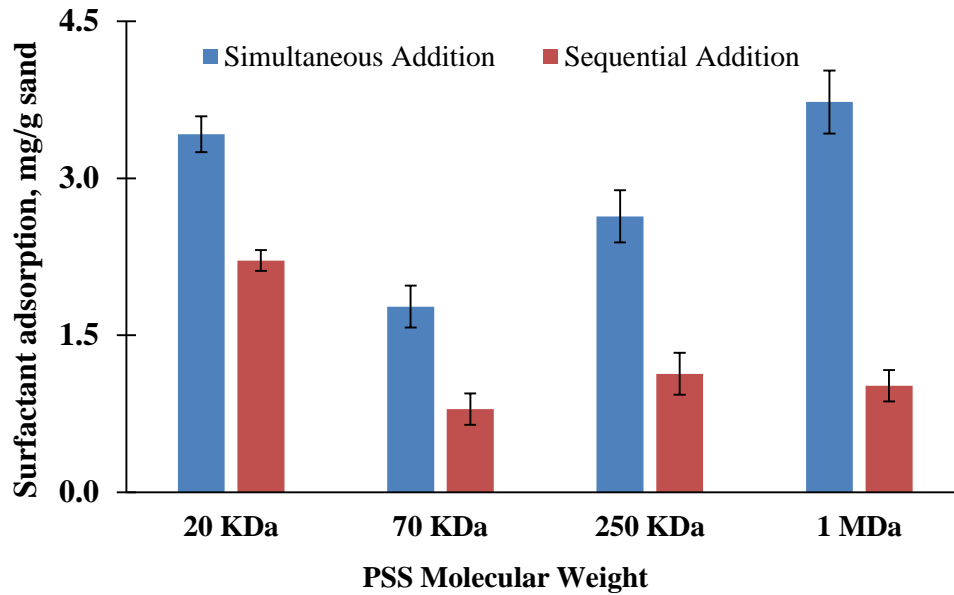


**Figure 18.** Effect of surfactant/PSS addition techniques on equilibrium adsorption of surfactant on Brea Sandstone in reservoir brine. PSS concentration is 0.4 wt. % and is based on the amount of sand.

The effects of surfactant/PSS addition techniques, sequential and simultaneous, on equilibrium adsorption of surfactant are shown in Figure 18. The results used for comparison are obtained at 0.4 wt % of PSSs. It is observed that the surfactant adsorption in the presence of each MW PSS is higher in the cases of simultaneous addition compared to sequential addition. This observation may be explained due to the fact that during sequential addition, polymers do not have to compete with surfactant to adsorb on solid surfaces. A similar phenomenon is also reported in the literature<sup>27</sup>. Figure 18 also shows that during simultaneous addition, 20 KDa SSMA and 1 MDa are found to be least effective in lowering surfactant adsorption. Such behavior of 20 KDa SSMA can be interpreted using similar explanations that are proposed for the observations made in

sequential addition. However, 1 MDa PSS has high surface charge density, doesn't contain MA, and is still less effective during simultaneous addition. This behavior may be the result of enormous difference between the molecular weights of 1 MDa PSS and surfactant. Generally, the smaller molecules diffuse faster than bigger molecules<sup>86</sup>. Therefore, during simultaneous addition, the slow diffusion rate of 1 MDa PSS may have prevented it from reaching the solid surfaces ahead of surfactant to block the adsorption sites for surfactant.

*Dynamic Adsorption of Surfactant without Polyelectrolyte*

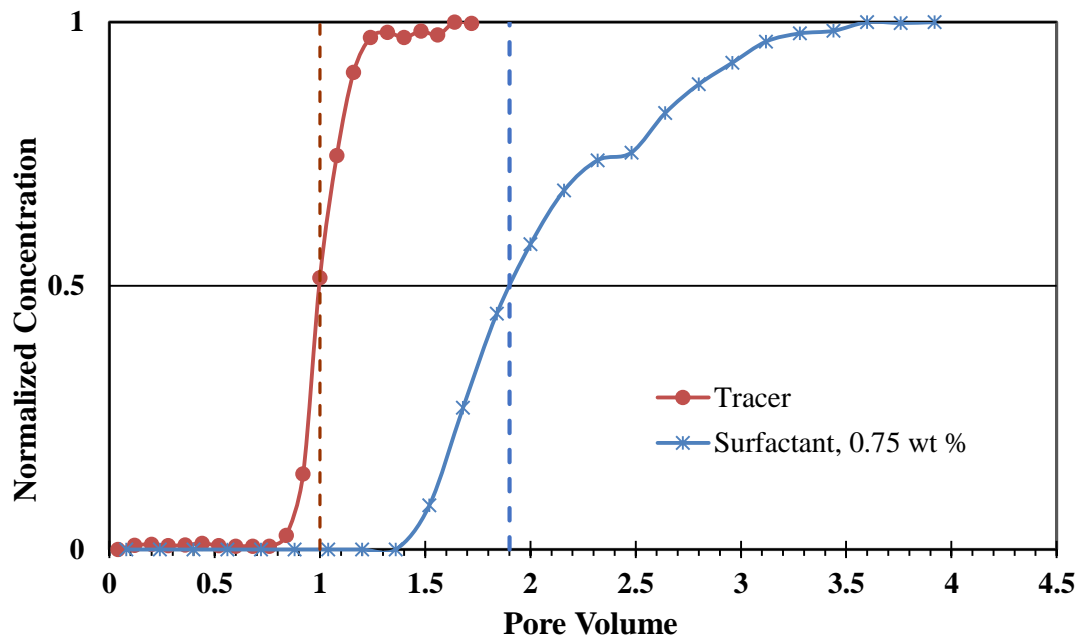


**Figure 19.** Dynamic surfactant adsorption in Brea sandstone packed bed at reservoir brine

Figure 15 shows that the equilibrium adsorption of surfactant without polyelectrolyte is severe on Brea sandstone from reservoir brine. This observation is further evaluated by conducting dynamic adsorption studies of surfactant without polyelectrolytes in packed beds of both crushed Brea sandstone and Ottawa sand. All the experiments are conducted

under reservoir brine, fluid injection rate is 0.3 mL/min, and the injected surfactant concentration is 0.75 wt %.

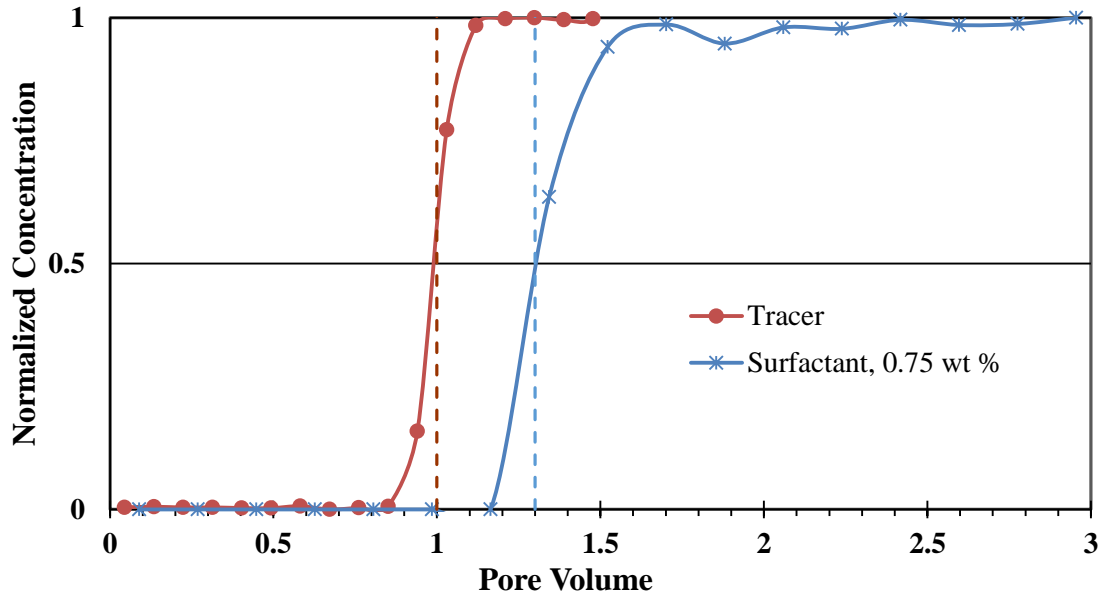


**Figure 20.** Dynamic surfactant adsorption in Ottawa sand packed bed at reservoir brine

Figure 19 shows the result of dynamic surfactant adsorption study performed on Brea sandstone. It can be seen that the surfactant breakthrough is at 1.9 PV indicating a total of 0.9 PV surfactant loss on solid surfaces. The 0.9 PV delay in surfactant breakthrough corresponds to 1.81 mg/g sand of surfactant absorbed on Brea sandstone. This result is less than the equilibrium adsorption study that shows surfactant loss on Brea sandstone of about 5 mg/g sand. A possible explanation for such observation is the equilibration time. Several authors have studied the effect of equilibration time on surfactant adsorption and found that surfactant solution should be in contact with solid surface for at least 1 day to allow adsorption to reach completion<sup>19,27</sup>. Therefore, during dynamic adsorption study, short surfactant-sand contact time of about 2 h (24 to 30 h in equilibrium adsorption

study) from surfactant injection to breakthrough (1.9 PV) could have resulted in less surfactant adsorption.

The result of dynamic adsorption study conducted on Ottawa sand is shown in Figure 20. As shown in Figure 20, the surfactant breakthrough is observed at 1.3 PV. This suggests that the surfactant loss on Ottawa sand is 0.3 PV (0.49 mg/g sand) and is about 4 times less compared to the equilibrium surfactant adsorption on Brea sandstone that is shown in Figure 19. A similar trend, lower surfactant adsorption on Ottawa sand than on Brea sandstone, is also observed in equilibrium adsorption experiments and is shown in Figure 15. Moreover, the dynamic surfactant adsorption on Ottawa sand is 0.49 mg/g sand and is about half the equilibrium surfactant adsorption of 1.10 mg/g sand in reservoir brine. This further suggests that the short surfactant-sand contact time in dynamic study may not be sufficient for surfactant adsorption to reach completion.

#### *Dynamic Adsorption of Surfactant with Polyelectrolyte*

Efficiency of PSS as a sacrificial agent in lowering surfactant adsorption is further evaluated through dynamic adsorption experiments. These tests are performed in crushed Brea sandstone packed beds with reservoir brine by employing both sequential and simultaneous surfactant/PSS addition techniques. Moreover, the 70 KDa PSS that showed excellent result in equilibrium adsorption experiments is chosen as a test polyelectrolyte for dynamic tests.

Figure 21 & 22, show the result of dynamic adsorption study that was carried out by sequentially injecting PSS followed by surfactant. The injected concentration of both PSS and surfactant is 0.75 wt %. It is observed in Figure 21 that both PSS and surfactant exhibit delayed breakthrough at 1.3 PV and 1.5 PV compared to tracer at 1 PV. This



behavior is caused by the adsorption of both PSS and surfactant on sand surfaces. Most notable, in the presence of PSS, the surfactant breakthrough is 0.4 PV earlier compared to without PSS as shown in Figure 19 and 21. This earlier surfactant breakthrough indicates a reduction in adsorption and is attributed to the effectiveness of PSS in reducing surfactant adsorption by adsorbing on solid surfaces.

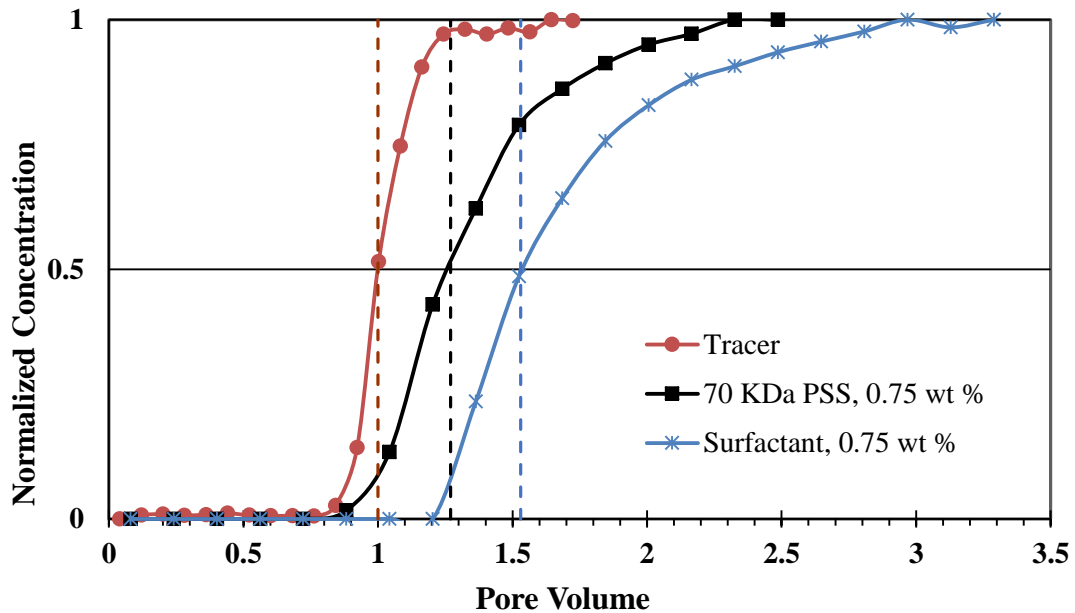


**Figure 21.** Effect of 70 KDa PSS on dynamic surfactant adsorption in Brea sandstone packed bed at reservoir brine. PSS and surfactant were injected sequentially

Figure 22 also shows the effect of surfactant/PSS addition techniques, sequential and simultaneous, on dynamic adsorptions of both surfactant and PSS. It is observed that the PSS adsorption is almost 2 times higher in sequential addition, about 0.50 mg/g sand, than in simultaneous addition, about 0.26 mg/g sand. This is because in sequential addition PSS may not have to compete with surfactant to adsorb on metal oxides. Normally, we expect higher PSS adsorption to lower surfactant adsorption and this corresponds very well with the observation made in Figure 22. It is observed that the

surfactant adsorption is about 1 mg/g sand in sequential addition and about 1.2 mg/g sand in simultaneous addition.

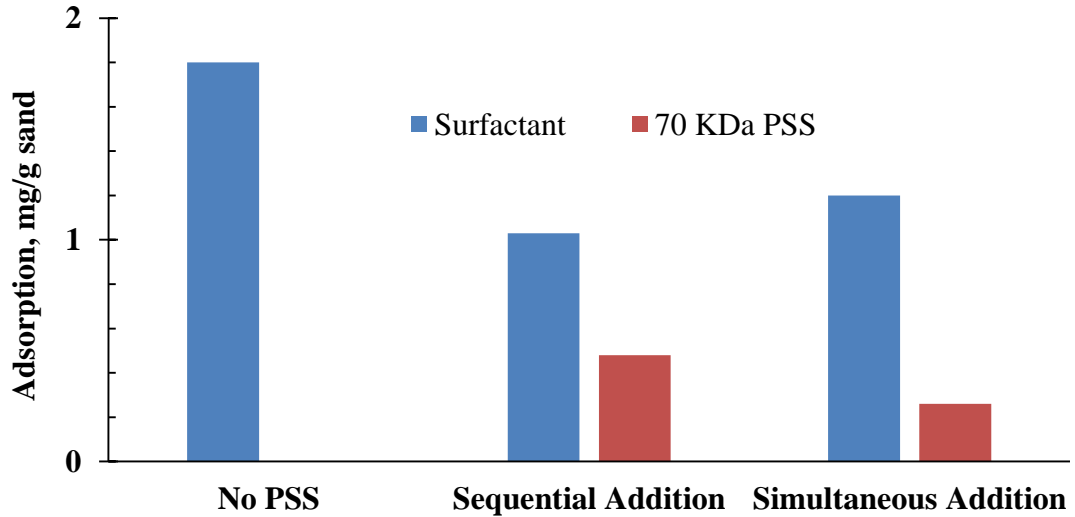


**Figure 22.** Effect of PSS/surfactant addition techniques on dynamic adsorption of surfactant and 70 KDa PSS in Brea sandstone packed bed at reservoir temperature

#### *Oil Mobilization in Sand Packs without Polyelectrolyte*

Two sand pack studies are conducted at reservoir conditions without polyelectrolyte in Ottawa and Brea packed beds to evaluate the effect of surfactant adsorption on oil mobilization. The tests include surfactant injection protocol of 1 PV, 0.75 wt %. Figures 23A and 23B compare the oil mobilization processes during surfactant injection in both Ottawa and Brea sand beds. It can be observed in Figure 23A that in the Ottawa sand packed bed, a distinct oil bank is formed after injecting 0.25 PV of surfactant. The oil bank continues to move towards the exit of the packed bed with the surfactant injection. Eventually, a clean sand pack is observed after post chemical water flooding, indicating mobilization of a majority of the trapped oil. However, a similar phenomenon is not observed in the case of the Brea sand packed bed. As shown in Figure 23B, even though

the formation of an oil bank is observed in Brea sand packed bed, it is not as distinct as the one observed in Ottawa sand packed bed and the oil bank stops moving towards the end of surfactant injection and doesn't move even after post surfactant water flooding.

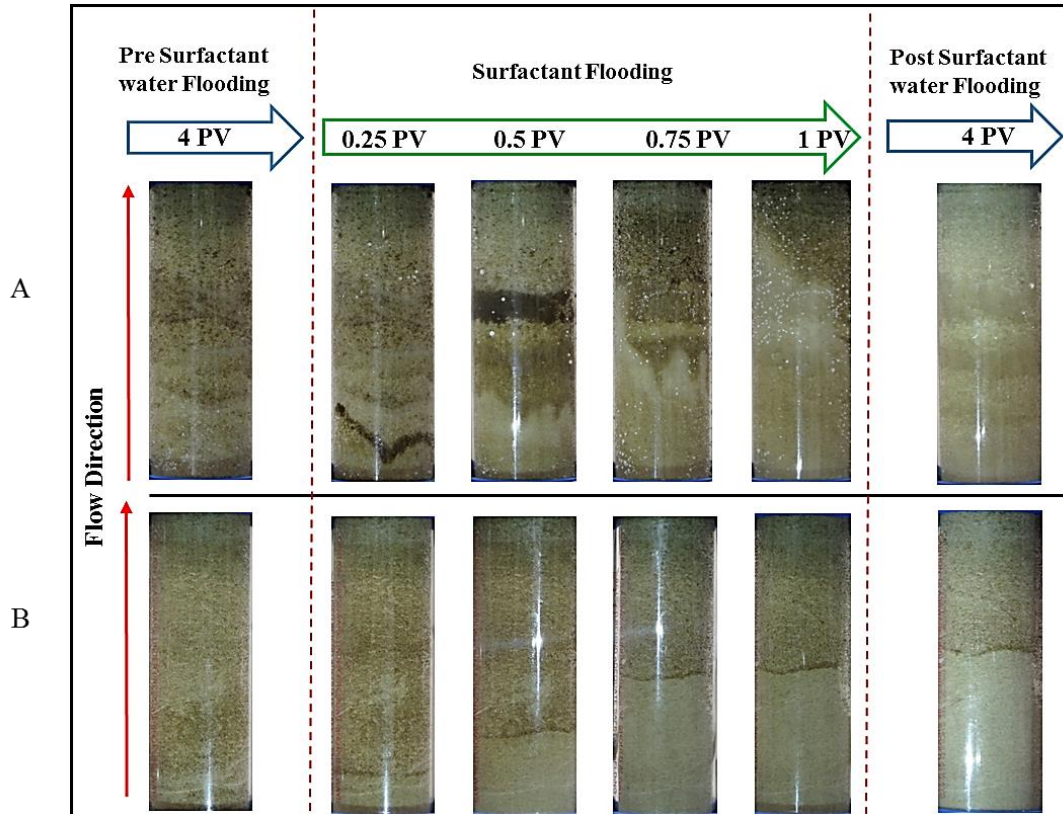


**Figure 23.** Sand pack studies conducted in (A) Ottawa sand and (B) Brea sandstone packed beds at the reservoir conditions ( $52^{\circ}\text{C}$ ) without polyelectrolyte. Surfactant injection protocol: 1 PV, 0.75 wt. %

Moreover, the amount of oil in effluents of each test is quantified. The results show about 60 % and 27% oil recovery from Ottawa bed and Brea bed respectively. Such difference in oil mobilization in two different sand packed beds is credited to the severe surfactant adsorption in Brea sandstone compared to Ottawa sand, which has been verified by both equilibrium and dynamic adsorption studies. Increased surfactant adsorption on soil/metal oxides negatively impacts oil displacement from porous media because the

adsorbed surfactant is not available to participate at oil-water interfaces to lower the IFT, which is the basis of cEOR.

*Oil Mobilization in Sand Packs with Polyelectrolyte*

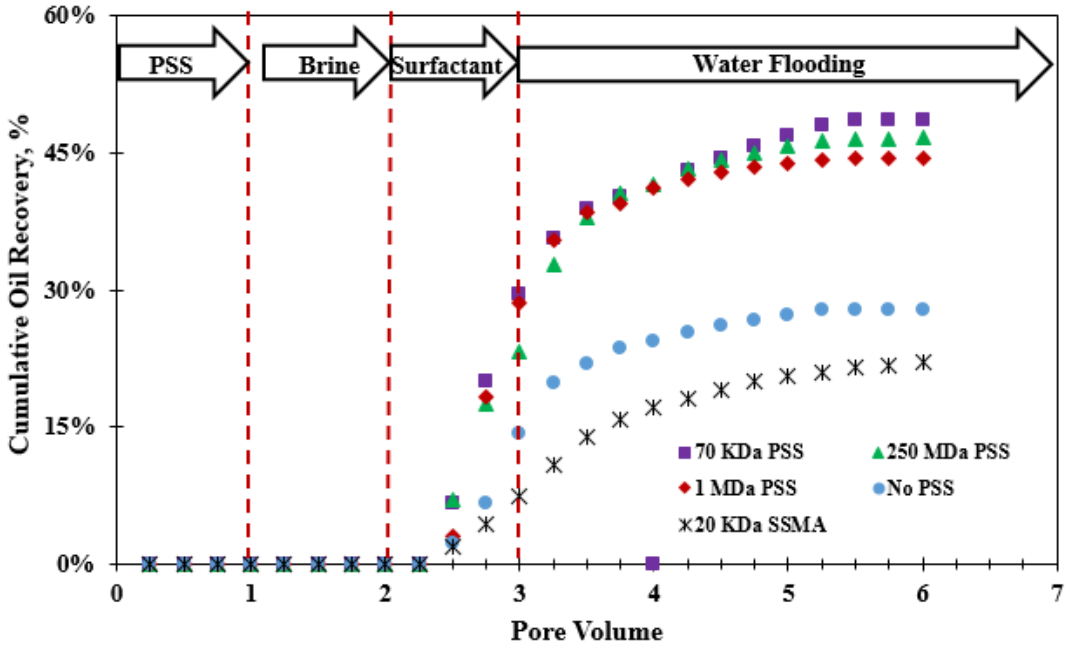


**Figure 24.** Sand pack studies in the presence of PSSs (1 PV, 0.4 wt. %) and Surfactant (1 PV, 0.75 wt. %) in Brea sandstone packed beds. Studies performed with reservoir brine at reservoir temperature of 52° C

The effect of PSSs on oil displacement by lowering surfactant adsorption is demonstrated through sand pack studies conducted in Brea packed beds. All four MW PSSs are evaluated and the sequential PSS/surfactant addition technique is employed for two reasons: First, both equilibrium and dynamic adsorption studies showed the sequential addition technique to be more effective in lowering surfactant adsorption. Second, PSS may interfere with the surfactant formulation. PSS is a hydrophilic compound and its addition to optimized surfactant formulation that is designed to form Type III microemulsion at reservoir conditions may shift the system towards Type I microemulsion, which is not desirable for cEOR. Therefore, after injecting PSS slug of 1

PV, 0.4 wt. %, sand packed beds are flushed with 1 PV of brine before injecting surfactant slug of 1 PV, 0.75 wt. %.

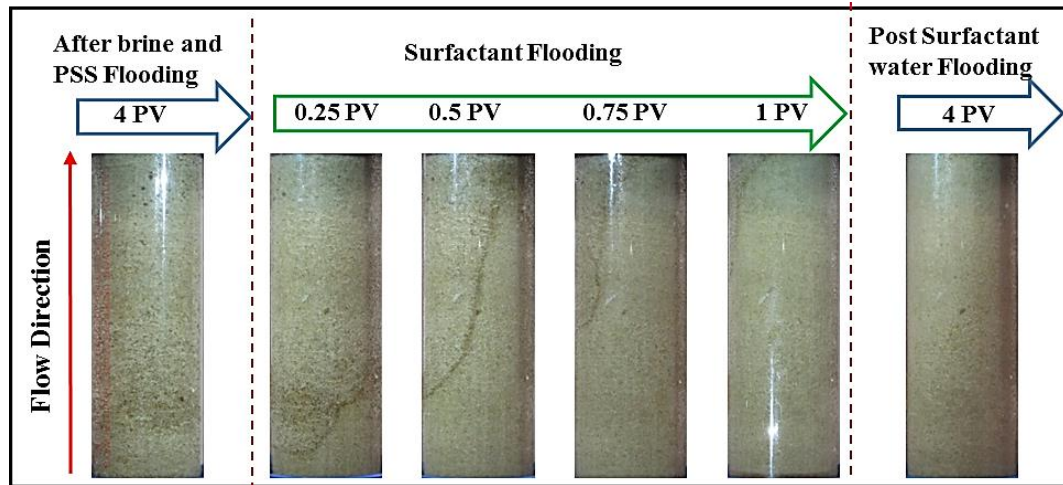


**Figure 25.** Effect of 70 KDa PSS (1 PV, 0.4 wt. %) on oil mobilization in Brea sandstone packed bed at reservoir condition (52° C). Surfactant injection protocol: 1 PV, 0.75 wt. %

Figure 24, shows the effect of PSS addition on cumulative oil recovery. It can be observed that in the case of 70 KDa PSS, the cumulative oil recovery is about 50 % which is almost two times more than the test without PSS. The observations made during oil displacement process of the test that includes 70 KDa PSS is shown in Figure 25. As observed in Figure 25, the formed oil bank continues to move with the surfactant injection and ultimately reaches the exit of the sand packed after post surfactant water flooding. This behavior is attributed to the role of 70 KDa PSS as a sacrificial agent in lowering surfactant adsorption. Figure 24 also shows that both 250 KDa and 1 MDa PSSs are nearly as effective as 70 KDa PSS in positively impacting oil recovery. These observations are consistent with equilibrium adsorption studies where all three PSSs lowered the surfactant adsorption by similar quantities as shown in Figure 18. In addition, Figure 25 shows that 20 KDa SSMA negatively impacts oil recovery. This behavior is unusual because equilibrium adsorption studies show that 20 KDa SSMA lowers surfactant adsorption

even though it is not as effective as other three MW PSSs. A possible explanation may be the wettability alteration. Addition of a thousand ppm of 20 KDa SSMA in brine is found to decrease brine pH from 6.5 to 5.6. It is reported that decrease in pH makes sandstone rock more oil wet which negatively impacts oil recovery<sup>87</sup>. Therefore, the pH decreasing tendency of 20 KDa SSMA may have made sandstone rock more oil wet and thus may have negatively affected oil recovery.

The effect of PSS concentration on oil recovery is also studied and is shown in Figure 26.

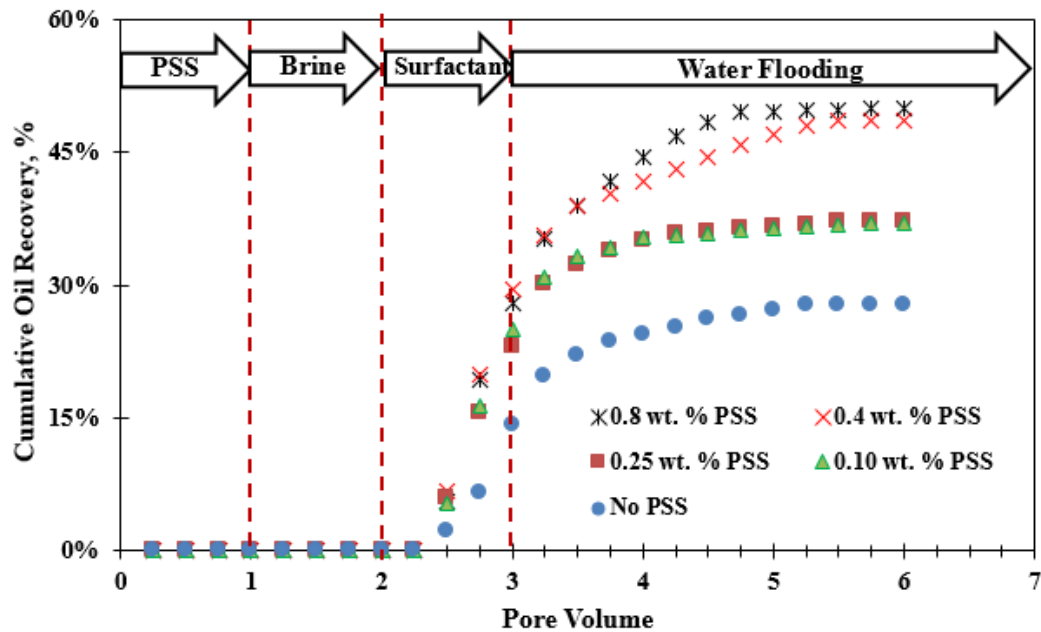


**Figure 26.** Effect of PSS (70 KDa) concentration on oil recovery from Brea sandstone packed beds at reservoir condition (52° C). Surfactant injection protocol: 1 PV, 0.75 wt. %

It is observed that the oil recovery increases with the 70 KDa PSS concentration. However, no significant difference in oil recovery is observed in the cases of 0.4 wt % and 0.8 wt %. This suggest that injecting PSS slug that contains more than 0.4 wt % of PSS does not make a significant difference in lowering surfactant adsorption. A similar observation is also made in equilibrium adsorption studies.

## Conclusions

This work demonstrates the polyelectrolyte, polystyrene sulfonate, to be a promising sacrificial agent for reservoirs containing extremely high TDS brine. The equilibrium surfactant adsorption studies without PSS show severe surfactant adsorption on Brea sandstone under high saline environment. However, after adding PSS, the surfactant adsorption is decreased by more than half. Among four different MW PSSs, the 70 KDa is found to be the most effective while 20 KDa SSMA is the least effective in decreasing surfactant adsorption. The presence of MA block in 20 KDa SSMA is thought to decrease its overall effectiveness by lowering the solution pH. The equilibrium adsorption studies also illustrate that even though 250 KDa and 1 MDa PSSs adsorb less on Brea sandstone compared to 70 KDa PSS, they are as effective as 70 KDa PSS in lowering surfactant adsorption. High surface charge density of high MW polymers is attributed for such observation.

The dynamic adsorption tests show lower surfactant adsorption compared to equilibrium adsorption studies. This could be the result of short surfactant-sand contact time of about 2 h in dynamic tests. Additionally, the sequential surfactant/PSS addition technique is found to be more effective than the simultaneous addition technique. This observation further verifies the hypothesis proposed by Weston et al. that during sequential addition, PSS does not have to compete with surfactant to adsorb on solid surfaces.

The sand pack study performed without PSS in a crushed Brea sandstone packed bed shows less than half the recovery compared to the test performed in Ottawa sand packed bed. Also, the oil recovery is found to double in a Brea sand packed bed in the presence of PSS indicating its effectiveness in lowering surfactant adsorption resulting in improved oil recoveries. However, 20 KDa SSMA is found to negatively impact oil recovery. The

hypothesis proposed for such observation is that 20 KDa SSMA, which lowers the brine pH, could have increased the oil wet nature of Brea sandstone. Additionally, 70 KDa, 250 KDa, and 1 M PSSs are found to have similar effect on oil recovery suggesting their potential application in cEOR as a sacrificial agent.



## **CHAPTER 5: Conclusions, Implications and Future Works**

The motivation of this chapter is to highlight important findings of previous three chapters and to show how those findings relate to the objectives of this dissertation. This chapter also addresses any shortcomings or limitations of the techniques/principles observed during this research and recommends future work that needs to be done in order to understand or overcome those limitations. Additionally, the potential uses and implications of these findings in other areas of research are also discussed. The overall objectives of this research were to develop a robust surfactant formulation for reservoir containing extremely high TDS brine, to study the viability of HLD method in cEOR, and to test PSSs as a sacrificial agent in minimizing surfactant adsorption on rock surfaces in high TDS Brine.

In Chapter 2, alcohol free binary mixtures of sodium alkyl alkoxy sulfates, extended surfactant, and sodium alkyl ethoxy sulfates, SAES, are demonstrated to be a promising basis for surfactant formulation for an extremely high TDS brine. The proposed surfactant formulations meet several criteria of a robust cEOR surfactant formulations. The only limitation of these formulations is that they can only be used in low temperature ( $< 60^{\circ}\text{C}$ ) reservoirs because the sulfate head groups of both extended and SAES hydrolyzes above  $60^{\circ}\text{C}$ . Therefore, future work is recommended to explore surfactants that are suitable for both extremely high TDS and high temperature reservoir conditions. One possible alternative is to use surfactants that have high temperature resistant sulfonate or carboxylate head groups coupled with high salinity resistant polar groups (ethylene oxides and propylene oxides).

Chapter 2 also shows that the HLD method can be used as a surfactant pre-screening tool for cEOR. Unlike quantitative structure-property relationship (QSPR) technique, the

HLD method takes into account the reservoir conditions and accurately predicts ratio between two surfactant at which the optimal Type III microemulsion could form. The only drawback of the HLD method is that it cannot determine the aqueous phase stability of the proposed formulation at the formulation condition. Therefore further study is recommended and perhaps the separate studies of surfactant precipitation boundaries and coacervation may provide some insight. In addition, the correct determination of the HLD parameters such as surfactant head constant, K-value, and temperature parameter,  $\alpha_T$ , are found to govern the accuracy of such correlation. As discussed in chapter 2, it is not possible to determine such parameters for surfactants that do not form clear middle phase microemulsion. Therefore, further study is recommended to explore the techniques that can precisely determine the K-value and  $\alpha_T$  value of all surfactant class/family. Perhaps, in theory, this issue could be addressed by mixing surfactant of interest with reference surfactant, AMA, that can form middle phase with variety of oils, constructing graphs of  $\ln S^*_{\text{mix}}$  against EACN and  $\ln S^*_{\text{mix}}$  against  $\Delta T$ , and applying linear surfactant mixing rule as reported by Acosta *et al.*<sup>45</sup>. Moreover, the HLD concept, which describes microemulsion systems, has been around for nearly three decades but its practical application is still limited. One possible reason for this may be the lack of technique which can accurately determine HLD parameters of majority of surfactants. Therefore, developing such a method may also expand the implication of HLD method in other areas of microemulsions such as drug delivery, detergency, personal care products, and so forth.

Chapter 3 investigates the field feasibility of the surfactant formulations discussed in chapter 2. The field test was conducted at the oil field site located near Guymon,

Oklahoma. During this test, SWTTs were implemented before and after surfactant injection to assess the effectiveness of laboratory optimized surfactant formulation. The numerical simulation method applied to interpret field data show 73% Sor reduction after surfactant injection suggesting the viability of proposed formulation in high TDS condition. Although the single well field test is found to be successful in mobilizing residual oil, some unpublished data show a very low success rate of the surfactant-only flooding in full scale inter-well tests. A possible explanation may be the severe surfactant adsorption onto the reservoir rocks which is further addressed in chapter 4.

Finally, chapter 4 relates the surfactant adsorption with the high salinity brine and its impact on oil mobilization. It also investigates the effectiveness of polyelectrolyte, PSS, as a sacrificial agent to minimize adsorption of anionic surfactant on oppositely charged rock surface in high salinity brine. Results show that after adding PSS, the surfactant adsorption on Brea sandstone is significantly minimized. In addition, sand pack studies conducted in the presence of PSS show improved oil recovery with surfactant-only flooding in high TDS brine suggesting the future of PSS as a promising sacrificial agent for cEOR. The other factor that could improve oil recovery is the viscosity of injection slug. Increasing the viscosity of injection solution reduces the fingering effect, improves mobility ratio, and ensure uniform oil displacement which ultimately increases oil recovery. Traditionally, bio-polymers and polyacrylamide are used to increase the viscosity of the injection water/surfactant slug in cEOR. However, these polymers cannot withstand high TDS brine. Therefore, further research needs to be done to explore polyelectrolytes that not only reduce surfactant adsorption but also increase viscosity at high salinity condition.

In chapter 4, the efficiency of PSS in reducing the surfactant adsorption and its effect on oil mobilization are evaluated through sand pack studies. These sand pack studies are conducted by taking into account two reservoir properties such as temperature and brine salinity. However other properties such as formation rock permeability and pressure may affect the performance of both surfactant formulation and PSS. Therefore, coreflood studies, which can simulate the reservoir conditions, are recommended in order to gain in-depth understanding of the proposed systems.

Currently, there is a growing interest and need for a chelating agent, which is inexpensive and effective, for oil field applications, especially in offshore opportunities. This is because industries prefer to make use of seawater and avoid installation of water hardness softening facility to lower the overall cost of project. Usually seawater contains high amount of divalent and monovalent metal ions which may lead to the precipitation of vital components such as alkali, surfactant, polymers, and so forth from the injection fluid and thus makes it ineffective. As discussed in chapter 4, PSSs show increased hardness tolerance and have high charge density especially in high molecular weight PSS. The high molecular weight PSSs, 250 KDa and 1 MDa, are relatively cheaper, about \$1.75/lb, compared to low molecular weight PSS, 70 KDa, which is about \$5.0/lb (information provided by the supplier). Therefore, future study is recommended to evaluate the effectiveness of high molecular weight PSS as a chelating agent in hard water. Applications such as offshore hydraulic fracking<sup>88</sup> and flow assurance<sup>89</sup> could benefit from this research.

## References

- (1). Zitha, P.; Felder, R.; Zornes, D.; Brown, K.; Mohanty, K., Increasing hydrocarbon recovery factors. *SPE Technol. Updates* **2011**.
- (2). Lake, L. W.; Venuto, P. B., A niche for enhanced oil recovery in the 1990s. *Oil & Gas Journal* **1990**, 88 (17), 62-67.
- (3). Melrose, J., Role of capillary forces in detennining microscopic displacement efficiency for oil recovery by waterflooding. *Journal of Canadian Petroleum Technology* **1974**, 13 (04).
- (4). Morrow, N. R., Interplay of capillary, viscous and buoyancy forces in the mobilization of residual oil. *Journal of Canadian Petroleum Technology* **1979**, 18 (03).
- (5). Morrow, N.; Chatzis, I.; Taber, J., Entrapment and mobilization of residual oil in bead packs. *SPE Reservoir Engineering* **1988**, 3 (03), 927-934.
- (6). Schramm, L. L., *Surfactants: fundamentals and applications in the petroleum industry*. Cambridge University Press: 2000.
- (7). Hirasaki, G.; Miller, C. A.; Puerto, M., Recent advances in surfactant EOR. *SPE Journal* **2011**, 16 (04), 889-907.
- (8). Möbius, D.; Miller, R.; Fainerman, V. B., *Surfactants: chemistry, interfacial properties, applications: chemistry, interfacial properties, applications*. Elsevier: 2001; Vol. 13.
- (9). Romsted, L. S., *Surfactant Science and Technology: Retrospects and Prospects*. CRC Press: 2014.
- (10). Ben Shiau, S.; Tzu-Ping Hsu, S.; Prapas Lohateeraparp, M. R.; Mahesh Budhathoki, A. R., Recovery of Oil from High Salinity Reservoir Using Chemical Flooding: From Laboratory to Field Tests. **2013**.
- (11). Puerto, M.; Hirasaki, G. J.; Miller, C. A.; Barnes, J. R., Surfactant systems for EOR in high-temperature, high-salinity environments. *SPE J* **2012**, 17 (1), 11-19.
- (12). Levitt, D. B.; Jackson, A. C.; Heinson, C.; Britton, L. N.; Malik, T.; Dwarakanath, V.; Pope, G. A., Identification and evaluation of high-performance EOR surfactants. *SPE Reservoir Evaluation & Engineering* **2009**, 2 (12), 243-253.
- (13). Sahni, V.; Dean, R. M.; Britton, C.; Kim, D. H.; Weerasooriya, U.; Pope, G. A. In *The role of co-solvents and co-surfactants in making chemical floods robust*, SPE Improved Oil Recovery Symposium, Society of Petroleum Engineers: 2010.

- (14). Noïk, C.; Bavière, M.; Defives, D., Anionic surfactant precipitation in hard water. *Journal of colloid and interface science* **1987**, *115* (1), 36-45.
- (15). Bansal, V.; Shah, D., The effect of divalent cations (Ca<sup>++</sup> and Mg<sup>++</sup>) on the optimal salinity and salt tolerance of petroleum sulfonate and ethoxylated sulfonate mixtures in relation to improved oil recovery. *Journal of the American Oil Chemists' Society* **1978**, *55* (3), 367-370.
- (16). Tabary, R.; Bazin, B.; Douarche, F.; Moreau, P.; Oukhemanou-Destremaut, F. In *Surfactant flooding in challenging conditions: Towards hard brines and high temperatures*, SPE Middle East Oil and Gas Show and Conference, Society of Petroleum Engineers: 2013.
- (17). Puerto, M. C.; Hirasaki, G. J.; Miller, C. A.; Reznik, C.; Dubey, S.; Barnes, J. R.; vanKuijk, S. In *Effects of Hardness and Cosurfactant on Phase Behavior of Alcohol-free Alkyl Propoxylated Sulfate Systems*, SPE Improved Oil Recovery Symposium, Society of Petroleum Engineers: 2014.
- (18). Krumrine, P. H.; Falcone Jr, J. S.; Campbell, T. C., Surfactant flooding 1: the effect of alkaline additives on IFT, surfactant adsorption, and recovery efficiency. *Society of Petroleum Engineers Journal* **1982**, *22* (04), 503-513.
- (19). ShamsiJazeyi, H.; Hirasaki, G. J.; Verduzco, R., Sacrificial Agent for Reducing Adsorption of Anionic Surfactants. *SPE-164061-MS* **2013**.
- (20). Wang, D.; Liu, C.; Wu, W.; Wang, G. In *Novel Surfactants that Attain Ultra-Low Interfacial Tension between Oil and High Salinity Formation Water without adding Alkali, Salts, Co-surfactants, Alcohols and Solvents*, SPE EOR Conference at Oil & Gas West Asia, Society of Petroleum Engineers: 2010.
- (21). ShamsiJazeyi, H.; Verduzco, R.; Hirasaki, G. J., Reducing adsorption of anionic surfactant for enhanced oil recovery: Part I. Competitive adsorption mechanism. *Colloids and Surfaces A: Physicochemical and Engineering Aspects* **2014**, *453*, 162-167.
- (22). Moreau, P.; Maldonado, A.; Oukhemanou, F.; Creton, B. In *Application of Quantitative Structure-Property Relationship (QSPR) Method for Chemical EOR Surfactant Selection*, SPE International Symposium on Oilfield Chemistry, Society of Petroleum Engineers: 2013.
- (23). Muller, C.; Maldonado, A. G.; Varnek, A.; Creton, B., Prediction of optimal salinities for surfactant formulations using a QSPR approach. *Energy & Fuels* **2015**.
- (24). Salager, J.; Morgan, J.; Schechter, R.; Wade, W.; Vasquez, E., Optimum formulation of surfactant/water/oil systems for minimum interfacial tension or phase behavior. *Soc. Pet. Eng. J* **1979**, *19* (2), 107-115.

- (25). Deans, H.; Carlisle, C. In *Single-well tracer test in complex pore systems*, SPE Enhanced Oil Recovery Symposium, Society of Petroleum Engineers: 1986.
- (26). Dobrynin, A. V.; Deshkovski, A.; Rubinstein, M., Adsorption of polyelectrolytes at an oppositely charged surface. *Physical review letters* **2000**, *84* (14), 3101.
- (27). Weston, J. S.; Harwell, J. H.; Shiau, B. J.; Kabir, M., Disrupting admicelle formation and preventing surfactant adsorption on metal oxide surfaces using sacrificial polyelectrolytes. *Langmuir* **2014**, *30* (22), 6384-6388.
- (28). Salager, J.-L.; Forgiarini, A. M.; Bullón, J., How to attain ultralow interfacial tension and three-phase behavior with surfactant formulation for enhanced oil recovery: a review. Part 1. Optimum formulation for simple surfactant–oil–water ternary systems. *Journal of Surfactants and Detergents* **2013**, *16* (4), 449-472.
- (29). Salager, J.-L.; Antón, R. E.; Sabatini, D. A.; Harwell, J. H.; Acosta, E. J.; Tolosa, L. I., Enhancing solubilization in microemulsions—state of the art and current trends. *Journal of surfactants and detergents* **2005**, *8* (1), 3-21.
- (30). Chiu, Y.; Hwang, H., The use of carboxymethyl ethoxylates in enhanced oil recovery. *Colloids and surfaces* **1987**, *28*, 53-65.
- (31). Stellner, K. L.; Scamehorn, J. F., Hardness tolerance of anionic surfactant solutions. 2. Effect of added nonionic surfactant. *Langmuir* **1989**, *5* (1), 77-84.
- (32). Cacace, M.; Landau, E.; Ramsden, J., The Hofmeister series: salt and solvent effects on interfacial phenomena. *Quarterly reviews of biophysics* **1997**, *30* (03), 241-277.
- (33). Minana-Perez, M.; Graciaa, A.; Lachaise, J.; Salager, J. In *Systems containing mixtures of extended surfactants and conventional nonionics. Phase behavior and solubilization in microemulsion*, Proceedings of 4th World surfactants congress, 1996; pp 226-234.
- (34). Witthayapanyanon, A.; Acosta, E.; Harwell, J.; Sabatini, D., Formulation of ultralow interfacial tension systems using extended surfactants. *Journal of surfactants and detergents* **2006**, *9* (4), 331-339.
- (35). Winsor, P. A., *Solvent properties of amphiphilic compounds*. Butterworths Scientific Publications: 1954.
- (36). Talley, L. D., Hydrolytic stability of alkylethoxy sulfates. *SPE Reservoir Engineering* **1988**, *3* (01), 235-242.

- (37). Lu, J.; Britton, C.; Solairaj, S.; Liyanage, P. J.; Kim, D. H.; Adkins, S.; Arachchilage, G. W.; Weerasooriya, U.; Pope, G. A., Novel large-hydrophobe alkoxy carboxylate surfactants for enhanced oil recovery. *SPE Journal* **2014**, (Preprint).
- (38). Yang, H.; Britton, C.; Pathma, J. L.; Solairaj, S.; Kim, D. H., Low-cost, high-performance chemicals for enhanced oil recovery. In *In SPE Improved Oil Recovery Symposium*, Society of Petroleum Engineers: 2010.
- (39). Shiau, B. J. B.; Harwell, J. H.; Lohateeraparp, P.; Dinh, A. V.; Roberts, B. L.; Hsu, T.-P.; Anwuri, O. I. In *Designing alcohol-free surfactant chemical flood for oil recovery*, SPE EOR Conference at Oil & Gas West Asia, Society of Petroleum Engineers: 2010.
- (40). Sanz, C.; Pope, G. In *Alcohol-free chemical flooding: from surfactant screening to coreflood design*, Paper SPE 28956, presented at the International Symposium on Oilfield Chemistry, San Antonio, Texas, 1995; pp 14-17.
- (41). Hsu, T.-P.; Prapas, L.; Wang, X.; Budhathoki, M.; Shiau, B. B., Improved oil recovery by chemical flood from high salinity reservoirs-single-well surfactant injection test. In *In SPE EOR Conference at Oil and Gas West Asia*, Society of Petroleum Engineers: 2012.
- (42). Davies, J. In *A quantitative kinetic theory of emulsion type, I. Physical chemistry of the emulsifying agent*, Gas/Liquid and Liquid/Liquid Interface. Proceedings of the International Congress of Surface Activity, 1957; pp 426-438.
- (43). Skauge, A.; Fotland, P., Effect of pressure and temperature on the phase behavior of microemulsions. *SPE Reservoir Engineering* **1990**, 5 (04), 601-608.
- (44). Ghosh, S.; Johns, R. T. In *A New HLD-NAC Based EOS Approach to Predict Surfactant-Oil-Brine Phase Behavior for Live Oil at Reservoir Pressure and Temperature*, SPE Annual Technical Conference and Exhibition, Society of Petroleum Engineers: 2014.
- (45). Acosta, E. J.; Yuan, J. S.; Bhakta, A. S., The characteristic curvature of ionic surfactants. *Journal of Surfactants and Detergents* **2008**, 11 (2), 145-158.
- (46). Trahan, G.; Nguyen, T.; Jakobs-Sauter, B. In *Applying the Hydrophilic–Lipophilic Deviation (HLD) Concept to Chemical EOR Formulations*, IOR 2015-18th European Symposium on Improved Oil Recovery, 2015.
- (47). Witthayapanyanon, A.; Harwell, J.; Sabatini, D., Hydrophilic–lipophilic deviation (HLD) method for characterizing conventional and extended surfactants. *Journal of colloid and interface science* **2008**, 325 (1), 259-266.



- (48). Hammond, C. E.; Acosta, E. J., On the characteristic curvature of alkyl-polypropylene oxide sulfate extended surfactants. *Journal of Surfactants and Detergents* **2012**, *15* (2), 157-165.
- (49). Velásquez, J.; Scorzza, C.; Vejar, F.; Forgiarini, A. M.; Antón, R. E.; Salager, J.-L., Effect of temperature and other variables on the optimum formulation of anionic extended surfactant–alkane–brine systems. *Journal of surfactants and detergents* **2010**, *13* (1), 69-73.
- (50). Rosen, M. J.; Kunjappu, J. T., *Surfactants and interfacial phenomena*. John Wiley & Sons: 2012.
- (51). Skauge, A.; Palmgren, O., Phase behavior and solution properties of ethoxylated anionic surfactants. *SPE* **1989**, *18499*, 355-366.
- (52). Antón, R.; Graciaa, A.; Lachaise, J.; Salager, J., Surfactant-oil-water systems near the affinity inversion part viii: optimum formulation and phase behavior of mixed anionic-nonionic systems versus temperature. *Journal of dispersion science and technology* **1992**, *13* (5), 565-579.
- (53). Kumar P, M. K., *Handbook of microemulsion science and technology*. Marcel Dekker: New York, 1999.
- (54). Flaaten, A.; Nguyen, Q. P.; Pope, G. A.; Zhang, J., A systematic laboratory approach to low-cost, high-performance chemical flooding. *SPE Reservoir Evaluation & Engineering* **2009**, *12* (05), 713-723.
- (55). Shah, D. O., and R.S. Schechter (eds), *Improved Oil Recovery by Surfactant and Polymer Flooding*. Academic Press: New York, 1977.
- (56). Rosen, M. J.; Wang, H.; Shen, P.; Zhu, Y., Ultralow interfacial tension for enhanced oil recovery at very low surfactant concentrations. *Langmuir* **2005**, *21* (9), 3749-3756.
- (57). Reed, R. L.; Healy, R. N., Some physicochemical aspects of microemulsion flooding: a review. *Improved Oil Recovery by Surfactant and Polymer Flooding* **1977**, 383-437.
- (58). Stegemeier, G. L. In *Relationship of Trapped Oil Saturation to Petrophysical Properties of Porous Media*, SPE Improved Oil Recovery Symposium, Society of Petroleum Engineers: 1974.
- (59). Maerker, J.; Gale, W., Surfactant flood process design for Loudon. *SPE reservoir engineering* **1992**, *7* (01), 36-44.

- (60). Jin, L.; Jamili, A.; Harwell, J. H.; Shiau, B.; Roller, C. In *Modeling and Interpretation of Single Well Chemical Tracer Tests (SWCTT) for pre and post Chemical EOR in two High Salinity Reservoirs*, SPE Production and Operations Symposium, Society of Petroleum Engineers: 2015.
- (61). Deans, H. Method of determining fluid saturations in reservoirs. 1971.
- (62). Deans, H.; Carlisle, C., *Single Well Chemical Tracer Test Handbook*. 1988.
- (63). Oyemade, S.; Al Harty, S.; Jaspers, H.; van Wunnik, J.; de Kruijf, A. In *Alkaline-surfactantpolymer flood: Single well chemical tracer tests-design, implementation and performance*. SPE 130042, Proc. SPE EOR conference at Oil & Gas West Asia, Muscat, Oman, 2010.
- (64). Deans, H. A.; Majoros, S. *Single-well chemical tracer method for measuring residual oil saturation. Final report*; Rice Univ., Houston, TX (USA): 1980.
- (65). De Zwart, A. H.; van Batenburg, D. W.; Stoll, M.; Al-Harthi, S. In *Numerical interpretation of single well chemical tracer tests for asp injection*, IOR 2011, 2011.
- (66). Hernandez, C.; Chacon, L.; Anselmi, L.; Angulo, R.; Manrique, E.; Romero, E.; de Audemard, N.; Carlisle, C. In *Single Well Chemical Tracer Test to Determine ASP Injection Efficiency at Lagomar VLA-6/9/21 Area C4 Member Lake Maracaibo Venezuela*, SPE/DOE Improved Oil Recovery Symposium, Society of Petroleum Engineers: 2002.
- (67). Jerauld, G.; Mohammadi, H.; Webb, K. J. In *Interpreting single well chemical tracer tests*, SPE Improved Oil Recovery Symposium, Society of Petroleum Engineers: 2010.
- (68). Seetharam, R.; Deans, H., CASTEM-A new automated parameter-estimation algorithm for single-well tracer tests. *SPE reservoir engineering* **1989**, 4 (01), 35-44.
- (69). Pope, G.; Wang, B.; Tsaur, K., A Sensitivity Study of Micellar/Polymer Flooding. *Society of Petroleum Engineers Journal* **1979**, 19 (06), 357-368.
- (70). Park, Y.; Deans, H.; Tezduyar, T., Thermal Effects on Single-Well Chemical-Tracer Tests for Measuring Residual Oil Saturation. *SPE Formation Evaluation* **1991**, 6 (03), 401-408.
- (71). Curbelo, F.; Garnica, A.; Neto, E. B., Enhanced oil recovery and adsorption of ionic surfactant. *Petroleum Science and Technology* **2013**, 31 (7), 663-671.
- (72). Somasundaran, P.; Hanna, H., Adsorption of sulfonates on reservoir rocks. *Society of Petroleum Engineers Journal* **1979**, 19 (04), 221-232.

- (73). O'Haver, J. H.; Jeffrey, H., Adsolubilization: some expected and unexpected results. *Surfactant adsorption and surface solubilization* **1995**, 615, 49-66.
- (74). Harwell, J. H.; Roberts, B. L.; Scamehorn, J. F., Thermodynamics of adsorption of surfactant mixtures on minerals. *Colloids and surfaces* **1988**, 32, 1-17.
- (75). Scamehorn, J.; Schechter, R.; Wade, W., Adsorption of surfactants on mineral oxide surfaces from aqueous solutions: I: Isomerically pure anionic surfactants. *Journal of Colloid and Interface Science* **1982**, 85 (2), 463-478.
- (76). Hankins, N. P.; O'Haver, J. H.; Harwell, J. H., Modeling effects of pH and counterions on surfactant adsorption at the oxide/water interface. *Industrial & engineering chemistry research* **1996**, 35 (9), 2844-2855.
- (77). Chandar, P.; Somasundaran, P.; Turro, N. J., Fluorescence probe studies on the structure of the adsorbed layer of dodecyl sulfate at the alumina—water interface. *Journal of colloid and interface science* **1987**, 117 (1), 31-46.
- (78). Trogus, F.; Schechter, R.; Wade, W., A new interpretation of adsorption maxima and minima. *Journal of Colloid and Interface Science* **1979**, 70 (2), 293-305.
- (79). ShamsiJazeyi, H.; Verduzco, R.; Hirasaki, G. J., Reducing adsorption of anionic surfactant for enhanced oil recovery: Part II. Applied aspects. *Colloids and Surfaces A: Physicochemical and Engineering Aspects* **2014**, 453, 168-175.
- (80). Paria, S.; Khilar, K. C., A review on experimental studies of surfactant adsorption at the hydrophilic solid—water interface. *Advances in colloid and interface science* **2004**, 110 (3), 75-95.
- (81). Kosmulski, M., pH-dependent surface charging and points of zero charge: III. Update. *Journal of Colloid and Interface Science* **2006**, 298 (2), 730-741.
- (82). Parks, G., Equilibrium concepts in natural water systems. *Advances in chemistry series* **1967**, 67, 121.
- (83). Parks, G. A., The isoelectric points of solid oxides, solid hydroxides, and aqueous hydroxo complex systems. *Chemical Reviews* **1965**, 65 (2), 177-198.
- (84). Somasundaran, P.; Krishnakumar, S., Adsorption of surfactants and polymers at the solid-liquid interface. *Colloids and Surfaces A: physicochemical and engineering aspects* **1997**, 123, 491-513.
- (85). Perrin, D., *pKa Prediction for Organic Acids and Bases*. Springer Science & Business Media: 2013.

- (86). Keyes, J. L., *Fluid, Electrolyte, and Acid-Base Regulation*. Jones & Bartlett Learning: 1990.
- (87). Aksulu, H.; Håmsø, D.; Strand, S.; Puntervold, T.; Austad, T., Evaluation of low-salinity enhanced oil recovery effects in sandstone: effects of the temperature and pH gradient. *Energy & Fuels* **2012**, 26 (6), 3497-3503.
- (88). Gidley, J. L., Recent advances in hydraulic fracturing. **1989**.
- (89). Islam, R., *Flow Assurance*. Wiley: 2015.